



105 SOUTH FOURTH STREET
ARTESIA, NEW MEXICO 88210
TELEPHONE (505) 748-1471

S. P. YATES
PRESIDENT
JOHN A. YATES
VICE PRESIDENT
B. W. HARPER
SEC. - TREAS.

December 12, 1986

Mr. R.L. Stamets, Director
New Mexico Oil Conservation Division
P.O. Box 2088
Santa Fe, New Mexico 87504-2088

Yates Petroleum Corp.
Freeman ACF No. 1
660' FSL & 660' FWL
Sec.22,T.16S.,R.37E.
Lea County, New Mexico

Gentlemen:

On August 28, 1986, Order No. R-8290 approved salt water disposal into the referenced well. The Order limits surface injection pressure to 500 psi, but contains a provision for the Director to raise the pressure limit by administrative process. Yates Petroleum Corporation hereby respectfully requests that the pressure limit be raised to 2100 psi.

The 500 psi limit was imposed due to concern that water disposed into the Freeman ACF No. 1 interval 10,050 to 10,350 might migrate to the Amerind Oil Carter No. 1 well located 810 feet FNL and 660 feet FEL Sec.28,T.16S., R.37E., enter the wellbore above the cement top at 10,200 feet, and travel uphole into fresh water zones. Section (5) of Order No. R-8290 allows the operator the opportunity to show why fresh water zones will not be disturbed by a higher disposal pressure, and to obtain administrative approval for a higher pressure. It is hoped that the following discussion of the attached information will convince the Director that an elevated operating pressure can be safely justified.

Attachment 1 is a report of a step rate test conducted by B & D Well Testers on the referenced well on November 18, 1986. This test revealed that fracture pressure of the disposal zone was reached when surface pressure was 2820 psi and disposal rate was 5000 barrels of water per day. The surface pressure, less pressure loss for tubing friction at this rate, was 2120 psi. This means that a surface disposal pressure of less than 2120 psi, plus whatever friction pressure occurs in the tubing for a given disposal rate, will not cause fracturing in the disposal zone. A surface disposal pressure of 2100 psi should not cause fracturing at any rate. Accordingly, this is the pressure now being requested for approval.

Attachment 2 is a map of the area surrounding the Freeman ACF No. 1. The main purpose of this map is to show nearby wells with zones that correlate with the Freeman ACF No. 1 disposal zones. As can be seen, the disposal zones are fairly extensive within the area.

Attachments 3 and 4 are cross sections of the disposal zones found in wells in the area. Attachment No. 3 shows the zones in wells within the "Area of Review," a one half mile radius circle around the Freeman ACF No. 1. Attachment 4 shows the zones in wells within most of the area covered by the map. Based on information revealed by Attachments 2 and 4, it is estimated that the disposal zones extend over an area of two and one half miles radius or greater.

Attachment 5 is a reservoir engineering study by William M. Cobb and Associates, Inc. wherein Dr. Cobb has determined the increase in pressure that can be expected to occur at the disposal zones in the Amerind Carter No. 1 as a function of time for different permeabilities. Permeabilities of 10, 50, and 100 millidarcies were used. These values were selected on the basis of how well the Freeman ACF No. 1 took water during the step rate test. The study assumes a constant disposal rate of 1000 barrels of water per day. Two cases are examined in the report, one for an infinite reservoir and one for a finite reservoir of two and one half miles radius. Tables 2 and 3 of the report give calculated pressure increases to be expected over periods of time ranging from six months to ten years.

Attachment 6 shows calculations of maximum allowable pressure increases at the disposal zones in the Amerind Oil Carter No. 1 under various constraints. These allowable increases are all based on an original reservoir pressure of 3,410 psi. This pressure comes from a drill stem test of the interval 10,160 feet to 10,198 feet in the Magnolia Petroleum Company Shipp No. 1 located 1980 feet FS&WL Sec.22,T.16S.,R.37E. This is the only available pressure measurement that could be found for the disposal zones. It is consistent with fluid levels found in the Freeman ACF No. 1 before disposal began.

The various constraints examined for allowable pressure increase consist of the amount of additional pressure required to lift a water column to the Ogollala at 275 feet, to the Santa Rosa at 1000 feet, to the Ogollala plus 1000 feet at 1275 feet, and to the Santa Rosa plus 1000 feet at 2000 feet. Because the Ogollala is a prolific aquifer and the Santa Rosa is a low probability water zone, the Ogollala plus 1000 feet limit is recommended as most reasonable. This limit will provide 1000 feet of margin for the Ogollala and 275 feet of margin for the Santa Rosa.

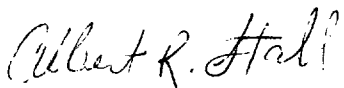
Attachment 7 is a graphic presentation of information contained in Dr. Cobb's study and maximum allowable pressure calculations in Attachment 6. It shows how long water can be disposed into the Freeman ACF No. 1 until the various pressure limits are reached at the Carter No. 1. Again, it is believed the most realistic limit would be the Ogollala plus 1000 feet. This means that a fluid level above 1,275 feet from the surface should not be allowed to occur. In the worst case, where a two and one half mile radius reservoir with 10 millidarcy permeability is considered, Attachment 7 shows water can safely be disposed for 5.8 years.

One last point worth mentioning is that all potential water zones are protected from the very beginning of the well by setting surface and intermediate casing string and circulating cement to surface. Attachment 8 reflects that surface and intermediate casing were set at 358 feet and 4200 feet, respectively, and circulated with cement in the Amerind Oil Carter No. 1.

In conclusion, we believe that elevating the surface disposal pressure at the Freeman ACF No. 1 to 2100 psi can be justified and your approval is requested.

Pursuant to Section (5) of Order R-8290, all mineral interest owners have been notified of this requested approval. Attachment 9 is a copy of the notification letter, and Attachment 10 is a list of owners notified by registered mail.

Sincerely,

Handwritten signature of Albert R. Stall in cursive script.

Albert R. Stall Engineer

cc: N.M.O.C.D., Hobbs

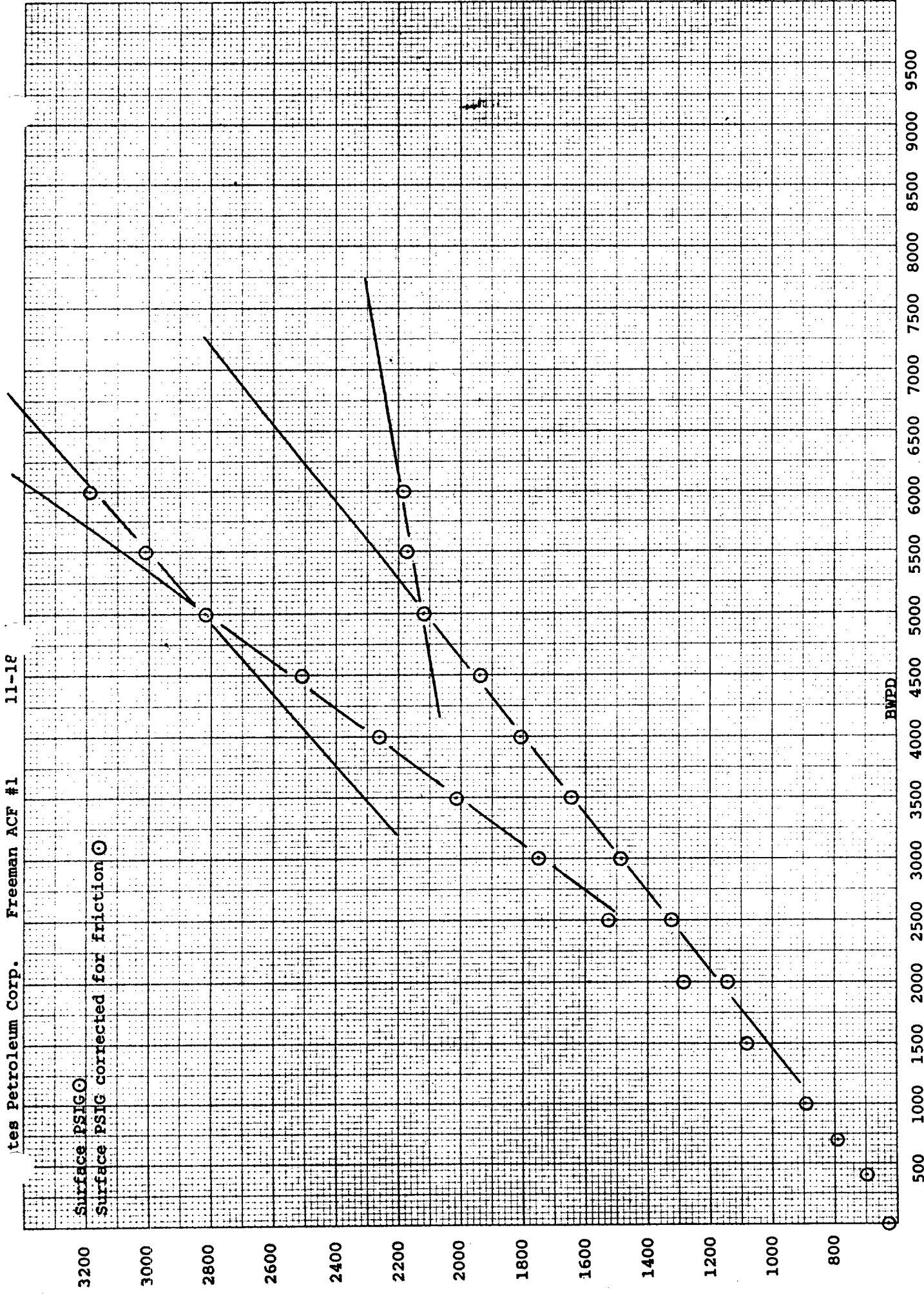
B & D WELL TESTERS

Step Rate Test

Phone (505) 397-3914

Hobbs, New Mexico 88240

Company Yates Petroleum						Test Date 11-18-86		Unit	
Total Depth						Plug Back TD		Elevation	
Csg size						Wt		Set at	
Tbg size						Wt		Set at	
Producing thru						Packer set at		Co. Rep Ray Stahl	
Time of Reading	Elap Time Hrs.	Well Information					Remarks		
		Rate BBLS Per Day	Total BBLS Per Rate	Surface PSIG	Surface PSI Cor for Friction	BHP			
10:15	Shut in			630					
10:20	Start	400		630					
10:25		400		685					
10:30		400		695					
10:35	:15	400	3.9	700					
10:40		700		765					
10:45		700		780					
10:50	:30	700	7.3	790					
10:55		1000		855					
11:00		1000		875					
11:05	:45	1000	10.2	895					
11:10		1500		1010					
11:15		1500		1050					
11:20	1:00	1500	15.4	1080					
11:25		2000		1205					
11:30		2000		1250					
11:35	1:15	2000	21.5	1280	1150		-130		
11:40		2500		1435					
11:45		2500		1480					
11:50	1:30	2500	25.4	1525	1325		-200		
11:55		3000		1635					
12:00		3000		1710					
12:05	1:45	3000	31.4	1755	1485		-210		
12:10		3500		1920					
12:15		3500		1975					
12:20	2:00	3500	36.3	2015	1645		-370		
12:25		4000		2175					
12:30		4000		2220					
12:35	2:15	4000	41.1	2260	1810		-450		



B & D WELL TESTERS, INC.

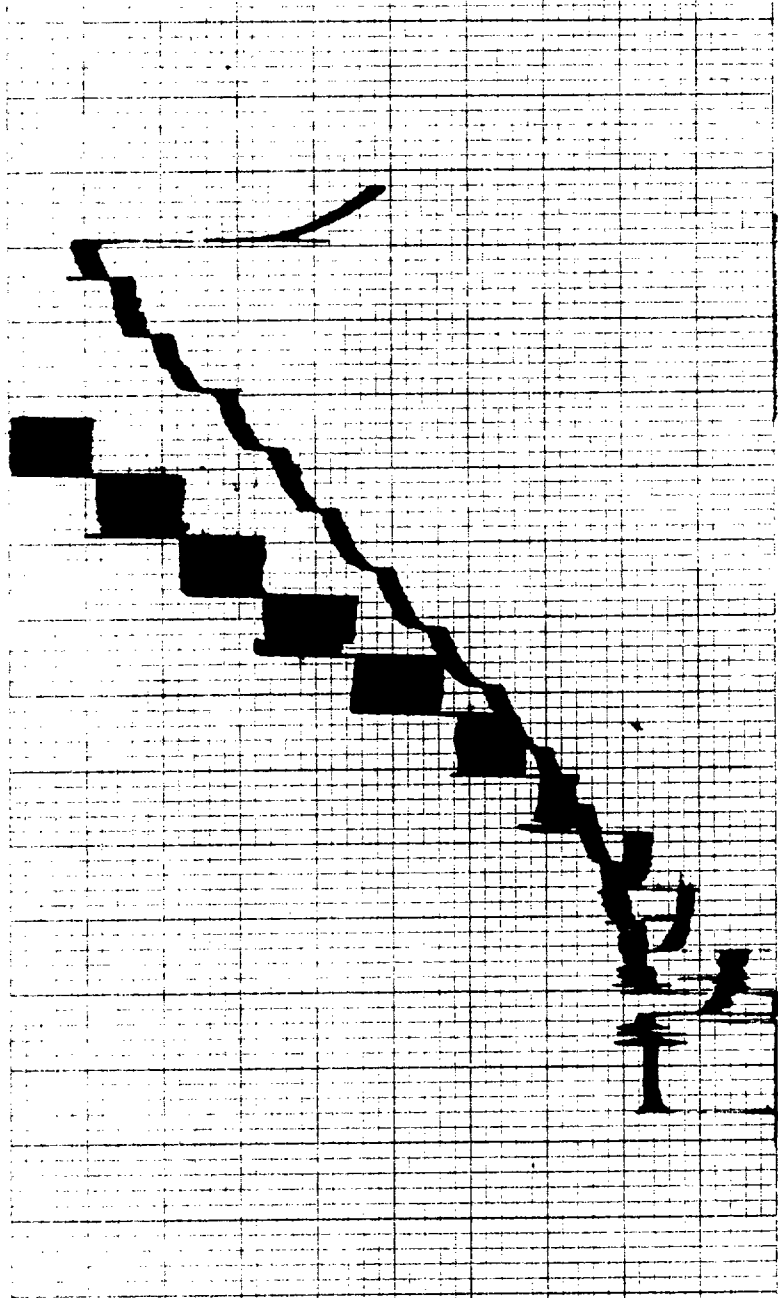
P.O. Box 5683
HOBBS, NEW MEXICO

505 397-3914

Yates Petroleum Corp.

Freeman ACF #1

11-18-86



NO. 59018

WILLIAM M. COBB & ASSOCIATES, INC.
Petroleum Engineering Consultants

907 North Central Plaza II
12770 Coit Road
Dallas, Texas 75251

December 3, 1986

(214) 385-0354

Mr. Ray Stall
Yates Petroleum Corporation
105 South 4th Street
Artesia, New Mexico 88210

Dear Ray:

At your request, we have calculated the anticipated pressure response at the Amerind Oil Company Carter Well No. 1 as a result of water injection into the Yates Petroleum Corporation Freeman "ACF" Well No. 1. Results are dependent upon injection rate, water viscosity, and several reservoir variables such as porosity, permeability thickness, areal extent, compressibility, and time. We have computed pressure response at various times for two different size reservoirs. Also, the effect of permeability on the pressure response was considered.

Table 1 lists values of reservoir variables which were used in the study. These parameters were obtained from Yates or from widely accepted petroleum industry correlations. With respect to reservoir size, the two cases considered assume that (1) the reservoir is unbounded (infinite acting) and (2) the reservoir is bounded (outer boundary closed to flow) at a radius of 2.5 miles.

Case 1 - Infinite Reservoir (Unbounded)

For an infinite acting reservoir, the pressure change at any position in the reservoir resulting from the injection at a single well at a constant rate can be determined using the line source solution to the diffusivity equation. The equation is described by Lee¹ and is

$$\Delta p(r,t) = \frac{70.6qBu}{kh} E_i \left(- \frac{\phi \mu c_t r^2}{0.00105kt} \right)$$

where

$\Delta p(r,t)$ = pressure change at any position, r , and any time, t

q = injection rate, BPD

B = formation volume factor, RB/STB

μ = viscosity, cp

k = effective permeability, md

h = formation thickness, ft.

ϕ = porosity, fraction

c_t = reservoir system compressibility, psi^{-1}

r = distance to point where Δp is measured, ft.

t = time at which Δp is measured, hrs.

E_i = exponential integral

For the parameters given in Table 1, Table 2 presents the pressure change at a position 1976' (the distance between the YPC injection well and the Amerind Oil Company Carter #1 well) for various levels of permeability. Figure 1 presents a semi-log graph of Δp versus k utilizing the data in Table 2.

Case 2 - Bounded Reservoir (Finite Reservoir)

For a closed outer boundary (bounded) reservoir, there is no simple analytical expression which is available for computing pressure changes at various positions. Fortunately, Earlougher, et al² published a paper in 1968 which provides information that can be used to compute pressure changes in rectangular shaped reservoirs. Since the actual geometry of the reservoir that is the subject of this study is not known, we have assumed the actual shape to be square with the injection well located at the center. Hence, the data in Reference 2 can be used to compute pressure changes at various points in the reservoir. Figure 2 presents a pictorial description of the reservoir utilized. As can be seen, when the distance from the YPC injection well to the nearest boundary is 13,200 feet (2.5 miles), the ratio of the distance between wells to the nearest boundary is 0.15 (1,976/13,200). (See Figure 2 of this report.) Consequently, on a dimensionless basis, the position of the Carter well in the square reservoir is at $X_D = 0.15$, $Y_D = 0.0$. (See Figure 1 of Reference 2.) With the position of the Carter well defined, actual pressure changes can be computed using the data in Table 1 of Reference 2. Consider the following example calculation utilizing Table 1 of Reference 2. First, it is necessary to define two terms.

$$t_{DA} = \frac{0.000264kt}{\phi\mu cA}$$

$$P_D = \frac{kh}{141.2qB\mu} * \Delta p$$

For the reservoir under investigation in this study, t_{DA} is related to actual time for a 10 md reservoir by

$$t_{DA} = \frac{(0.000264)(10)t}{(0.10)(0.50)(12 \times 10^{-6})(2 \times 13,200)^2}$$

$$t_{DA} = 0.00000631 * t$$

where t is measured in hours.

When $t = 4378$ hours (6 mos), $t_{DA} = 0.0276$.

Entering Table 1 of Reference 2, with t_{DA} of 0.0276 and interpolating between Column 1 ($X_D = 0$, $Y_D = 0$) and Column 3 ($X_D = 0.25$, $Y_D = 0$) using a graph of P_D versus X_D for $X_D = 0.15$ and $Y_D = 0$ yields a value of P_D of 1.575. For the reservoir under consideration

$$P_D = 1.575 = \frac{(10)(38)}{(141.2)(1000)(1)(0.5)} \Delta p$$

or $\Delta p = 293$ psi. This value of Δp represents the expected change in pressure at the Carter #1 after 6 months of injection.

Table 3 shows pressure changes at the Carter #1 well as a function of time for 3 levels of permeability. Figure 3 presents data in graphical form.

Summary

Ray, it would appear that the pressure change at the Carter well after 10 years of continuous injection of 1000 BHPD into the Yates well could range from less than 100 psi to about 1000 psi. If the net pay, porosity, or area are larger, then the pressure increases could be less.

After you have reviewed these materials, if any questions develop, give me a call. I appreciate the opportunity to again work with you and Dave Boneau.

Yours very truly,

Bill

William M. Cobb

WMC:cac

Ref. 1: Well Testing by John Lee, SPE Textbook Series Volume 1

Ref. 2: Earlougher, R.C., Jr., Ramey, H.J., Miller, F.G., and Mueller, T.D.: "Pressure Distributions in Rectangular Reservoirs" Trans. AIME - Vol. 243, 1968

TABLE 1

RESERVOIR AND FLUID PARAMETERS USED IN
PRESSURE RESPONSE CALCULATIONS AND SOURCE OF DATA

h = 38 feet (based on 10% porosity cutoff) - YPC

ϕ = 10% - WMC

μ = 0.5 cp - WMC

c_t = 12×10^{-6} /psi - WMC

B_w = 1.0 RB/STB - WMC

i_w = 1000 BHPD - YPC

r = 1976' - Distance between the YPC injection well and
the Amerind Oil Company well (the pressure response
point) - YPC

TABLE 2

PRESSURE CHANGE AT CARTER #1 AS A FUNCTION
OF TIME AND PERMEABILITY FOR INFINITE ACTING RESERVOIR

<u>Time</u>	<u>Permeability, md</u>		
	<u>10</u> <u>Δp, psi</u>	<u>50</u> <u>Δp, psi</u>	<u>100</u> <u>Δp, psi</u>
6 mos.	228	75	44
1 yr.	291	88	50
3 yrs.	390	108	60
5 yrs.	438	118	65
7.5 yrs.	475	125	69
10.0 yrs.	504	130	72

TABLE 3

PRESSURE CHANGE AT CARTER #1 AS A FUNCTION
OF TIME AND PERMEABILITY FOR A BOUNDED SQUARE RESERVOIR
WHCSE WIDTH IS 5.0 MILES (INJECTION RADIUS = 2.5 MILES)

<u>Time</u>	<u>Permeability, md</u>		
	<u>10</u> <u>Δp, psi</u>	<u>50</u> <u>Δp, psi</u>	<u>100</u> <u>Δp, psi</u>
6 mos.	293	92	62
1 yr.	353	125	95
3 yrs.	494	254	224
5 yrs.	623	383	353
7.5 yrs.	785	545	515
10.0 yrs.	946	707	676

FIGURE 2
DRAINAGE SHAPE FOR
BOUNDED RESERVOIR

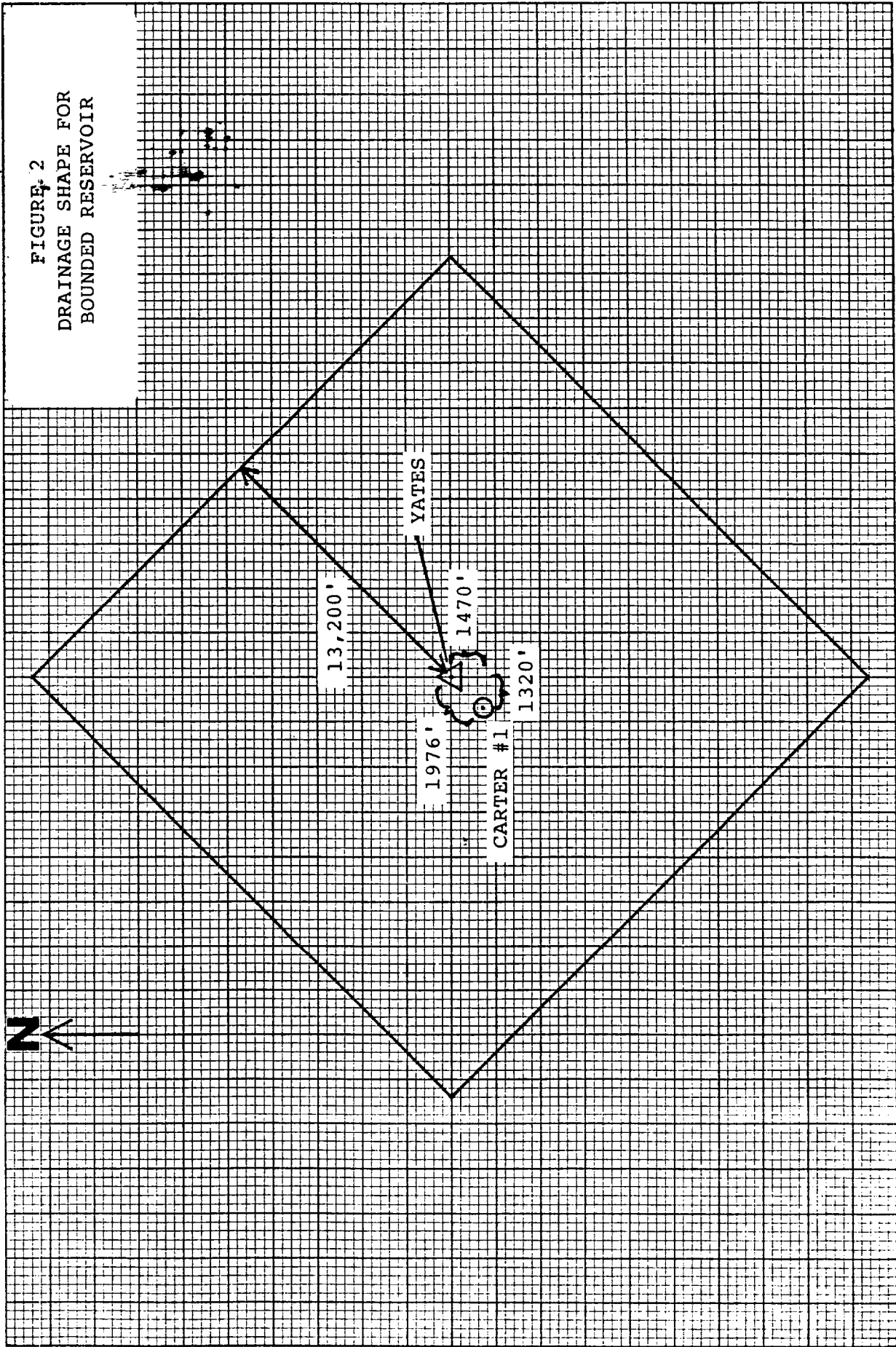
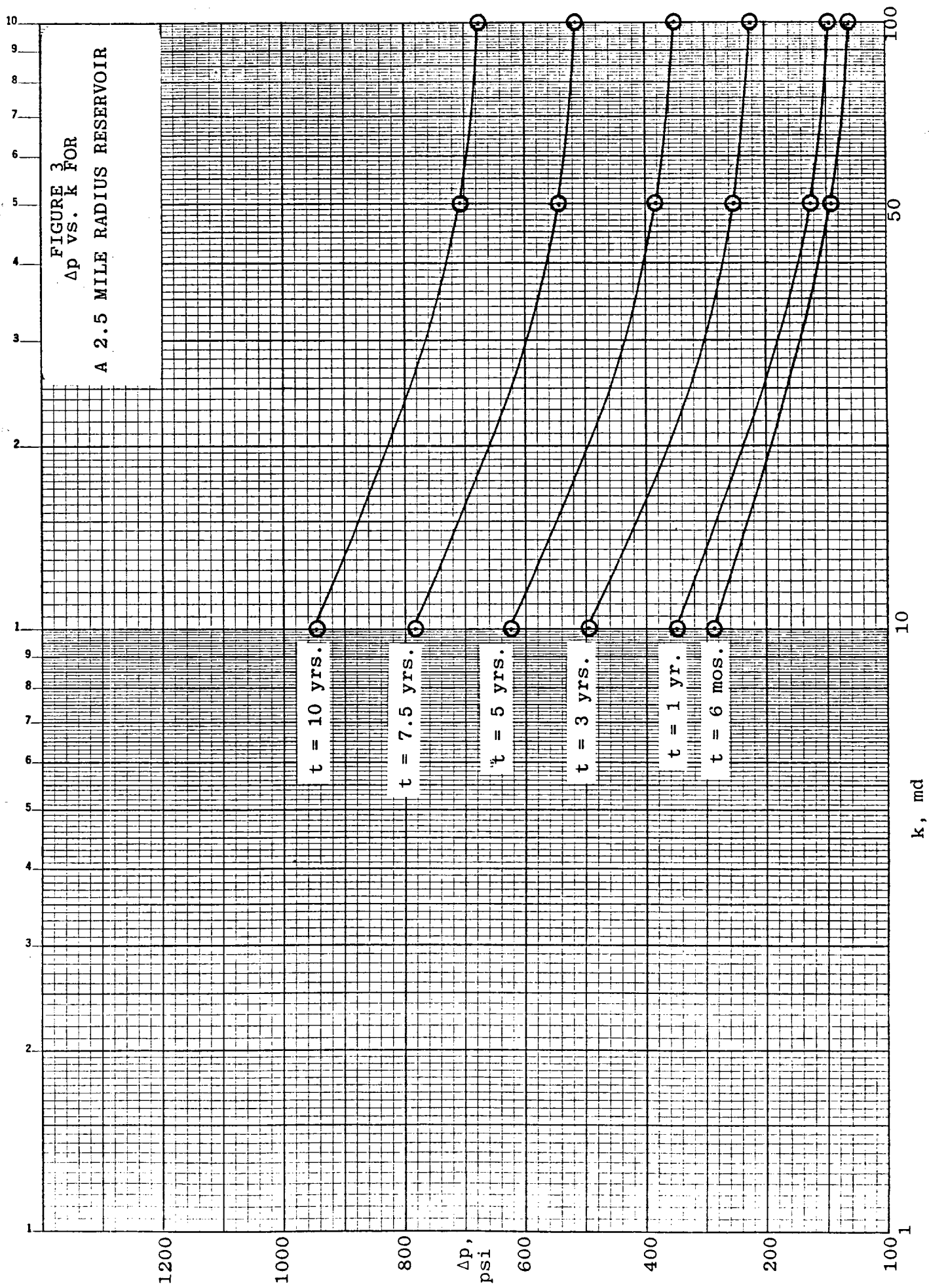


FIGURE 3
 Δp vs. k FOR
 A 2.5 MILE RADIUS RESERVOIR



Pressure Distributions in Rectangular Reservoirs

ROBERT C. EARLOUGHER, JR.
 JUNIOR MEMBER AIME
 H. J. RAMEY, JR.
 F. G. MILLER
 T. D. MUELLER
 MEMBERS AIME

MARATHON OIL CO.
 LITTLETON, COLO.
 STANFORD U.
 STANFORD, CALIF.
 STANDARD OIL CO. OF CALIFORNIA
 SAN FRANCISCO, CALIF.

Abstract

There are many studies of flow in radial systems that can be used to interpret unsteady reservoir flow problems. Although solutions for systems of infinite extent can be used to generate solutions for finite flow systems by superposition, application is tedious. In this paper a step is made toward simplifying calculations of such solutions for finite flow systems. Superposition is used to produce a tabulation of the dimensionless pressure drop function at several locations within a bounded square that has a well at its center. The square system provides a useful building block that may be used to generate flow behavior for any rectangular shape whose sides are in integral ratios. Values of the tabulated dimensionless pressure drop function are simply added to obtain the dimensionless pressure drop function for the desired rectangular system. The rectangular system may contain any number of wells producing at any rates. Furthermore, the outer boundaries of the rectangular system may be closed (no-flow) or they may be at constant pressure. Mixed conditions also may be considered. Tables of the dimensionless pressure drop function for the square system are presented and various applications of the technique are illustrated.

Introduction

In 1949 van Everdingen and Hurst¹ published solutions for the problem of water influx into a cylindrical reservoir. Since this problem is mathematically identical with the depletion of a cylindrical reservoir with a well at the origin, the van Everdingen-Hurst solution may be used to study the depletion problem. In their analysis, they assumed that the fluid had a small, constant compressibility such that flow was governed by the diffusivity equation

$$\frac{\partial^2 p}{\partial r^2} + \frac{1}{r} \frac{\partial p}{\partial r} = \frac{\phi \mu c}{k} \frac{\partial p}{\partial t} \quad (1)$$

For a constant production rate q starting at time zero, van Everdingen and Hurst showed that the unsteady pressure distribution for both finite and infinite systems could be expressed in terms of a dimensionless pressure

$$p_D(r_D, t_D) = \frac{2\pi k h (p_i - p)}{q\mu} \quad (2)$$

with

$$r_D = r/r_w \quad (3)$$

$$t_D = \frac{kt}{\phi \mu c r_w^2} \quad (4)$$

where r_w = wellbore radius (reservoir radius for influx)
 p_D = dimensionless pressure at r_D at t_D .

Tabulations of the dimensionless pressure drop for a unit value of r_D were provided by van Everdingen and Hurst,¹ and later by Chatas.² Others also presented values in graphical or tabular form.^{3,4} If the radius of the well becomes vanishingly small, $r_w \rightarrow 0$, the line source solution may be used for Eq. 2 when infinite systems are considered.

$$\begin{aligned} p_D(r_D, t_D) &= -\frac{1}{2} Ei \left(\frac{-\phi \mu c r^2}{4kt} \right) \\ &= -\frac{1}{2} Ei \left(\frac{-r_D^2}{4t_D} \right) \end{aligned} \quad (5)$$

where $-Ei(-x)$ is the well known exponential integral. If the argument of the exponential integral is small enough,

$$p_D(r_D, t_D) = -\frac{1}{2} \left[\ln \left(\frac{\phi \mu c r^2}{4kt} \right) + 0.5772 \right] \quad (6)$$

Eqs. 5 and 6 are excellent approximations for Eq. 2 under certain conditions.⁵

In 1954, Matthews, Brons and Hazebroek⁴ demonstrated that solutions such as Eq. 5 can be superposed to generate the behavior of bounded geometric shapes; i.e., the behavior of a bounded single-well system can be calculated by adding together the pressure disturbances caused by the appropriate array of an infinite number of wells producing from an infinite system. These wells are referred to as image wells. Matthews, Brons and Hazebroek considered systems containing a single well producing at a constant rate. This superposition can be represented analytically as

$$p_D(x_D, y_D, t_D) = \sum_{i=1}^{\infty} p_D(a_{iD}, t_D) \quad (7)$$

where $a_{iD} = a_i/\sqrt{A}$

a_i = distance from the i th well to the point (x_D, y_D)
 A = drainage area of the bounded system (which may be called the drainage area per well)

and

Original manuscript received in Society of Petroleum Engineers office July 6, 1967. Revised manuscript received Dec. 23, 1967. Paper (SPE 1956) was presented at SPE 42nd Annual Fall Meeting held in Houston, Tex., Oct. 1-4, 1967. © Copyright 1968 American Institute of Mining, Metallurgical, and Petroleum Engineers, Inc.

¹References given at end of paper.

$$t_{DA} = \frac{kt}{\phi\mu cA} t_D \left(\frac{r_w^2}{A} \right) \quad (8)$$

Here x_D and y_D are any convenient dimensionless coordinates. One useful set is given in Eqs. 13 and 14. The value $i = 1$ refers to the well within the bounded region under consideration.

The dimensionless time t_{DA} is particularly useful because a simple material balance (neglecting the wellbore volume) leads to the expression

$$\frac{2\pi kh(p_i - \bar{p})}{q\mu} = 2\pi t_{DA} \quad (9)$$

where \bar{p} is the average pressure within the drainage region. Also, a dimensionless time based on the drainage area is convenient for shapes other than circular as well as for circular shapes. In any event, any dimensionless time is simply a specific constant times real time, so conversion from one dimensionless time base to any other is an easy matter. However, it will be important to remember the dimensionless time basis when superposition is applied later in the paper. Henceforth, only the dimensionless time t_{DA} will be used.

Matthews, Brons and Hazebroek evaluated a function p_{DMBH} that is useful for correcting extrapolated pressure buildup data to average drainage area pressure.

$$p_{DMBH}(r_w, t_{DA}) = \frac{2\pi kh(p^* - \bar{p})}{q\mu} = 4\pi t_{DA} + \sum_{i=2}^{\infty} Ei \left(\frac{-a_{iD}^2}{4t_{DA}} \right) \quad (10)$$

where p^* is the pressure obtained by extrapolating the pressure buildup curve to infinite shut-in time. Note that i in the summation starts at 2, which means that a_i cannot equal r_w . Matthews, Brons and Hazebroek presented their results graphically for a wide variety of reservoir shapes (squares, rectangles, etc.). In addition to being useful for calculating drainage area average pressures, p_{DMBH} may be used to compute dimensionless pressure drop functions for pressure behavior at the well.

This study was conducted to find pressure-drop functions that may be used to determine pressure behavior for a variety of reservoir shapes, not only at the well but also at other locations of interest. In using these functions, the powerful superposition technique was employed in the simplest way. Properly selected columns of numbers were added together.

Pressure Distribution in a Square Drainage Shape

The problem considered initially was the unsteady depletion of a square drainage region with no-flow outer boundaries and a single well at the center. A thin, ideal, isotropic, homogeneous, horizontal formation containing a single-phase fluid of constant viscosity and compressibility was considered. Pressure gradients were assumed small such that second-degree gradient terms could be neglected. Gravitational forces were neglected. To generate the square drainage region, the method of superposition used by Matthews, Brons and Hazebroek⁶ was applied. Thus, Eq. 7 was used.

If (t_{DA}/a_{iD}^2) in Eq. 7 is as great as 20, the line source solution⁷ given in Eq. 5 may be used as an excellent approximation to $p_D(a_{iD}, t_{DA})$ for all values of a_i/r_w . For values of a_i/r_w as great as 250, the line source solution is within 0.1 percent of the finite cylinder source solution if

(t_{DA}/a_{iD}^2) is greater than 0.1 (see Figs. 3 and 4 of Ref. 5). Thus, for all practical situations, Eq. 7 may be written

$$p_D(x_D, y_D, t_{DA}) = -\frac{1}{2} \sum_{i=1}^{\infty} Ei \left(\frac{-a_{iD}^2}{4t_{DA}} \right) \quad (11)$$

For the case in which the dimensionless pressure drop at the producing well is calculated, the a_{iD} term for the producing well becomes r_w/\sqrt{A} . Since this term is small compared with other a_{iD} terms, Eq. 6 may be used for the producing well term. In this case Eq. 11 becomes

$$p_D(r_w, t_{DA}) = -\frac{1}{2} \left\{ \ln \left[\frac{r_w^2}{4At_{DA}} \right] + 0.5772 + \sum_{i=2}^{\infty} Ei \left(\frac{-a_{iD}^2}{4t_{DA}} \right) \right\} \quad (12)$$

Here the term for $i = 1$ has been dropped from the summation as it represents the production well that appears as the \ln term in Eq. 12.

The summation of exponential integrals in Eqs. 11 and 12 may be carried out by digital calculations, details of which were discussed by Matthews, Brons, and Hazebroek. Table 1 gives the results of using Eq. 11 to calculate the dimensionless pressure drop at the producing well and at 16 other points within a square drainage region with a well at the center. Fig. 1 shows the square grid used to generate Table 1. Because of the symmetry of the square drainage region, it is necessary to compute pressures only within the octant shown in Fig. 1. In the case of the pressure at the well, the calculations were carried out for $\sqrt{A}/r_w = 2,000$. These results may be converted to other \sqrt{A}/r_w values by

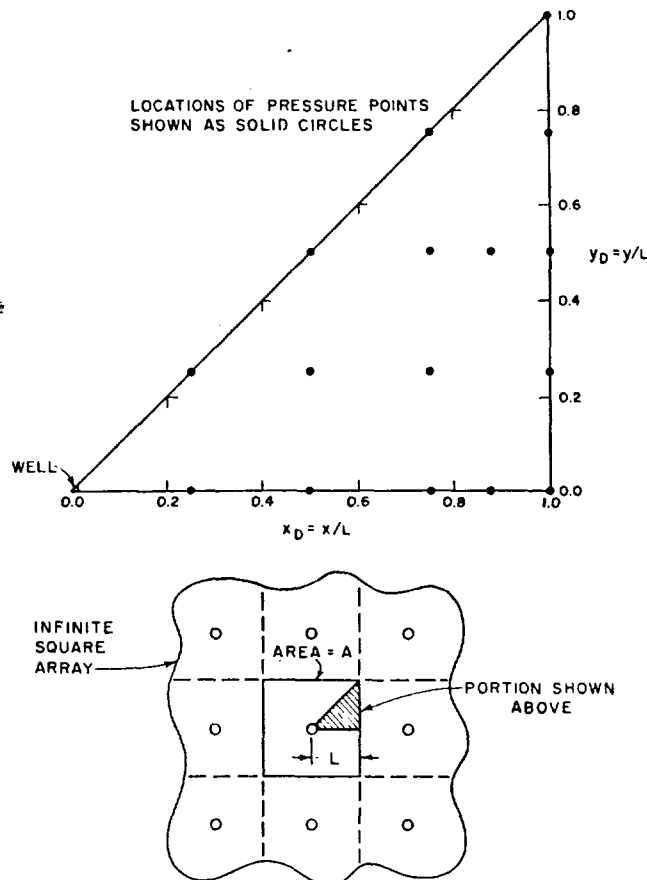


Fig. 1—Octant of a square drainage system showing well and pressure point locations.

means of Eqs. 11 or 12. To make this conversion the value of $-\frac{1}{2}[\ln(r_w^2/[4At_{Da}]) + 0.5772]$ would be subtracted from the tabulated values in Table 1, and the appropriate value of $p_D(r_{Dw}, t_{Da})$ substituted. The results for points

other than the well point are independent of the value of r_w for the conditions selected for this problem. Grid point pressures are sensitive to the value of \sqrt{A}/r_w for only small values of this ratio, and then at only very small t_{Da} .

TABLE 1—DIMENSIONLESS PRESSURES AS FUNCTIONS OF DIMENSIONLESS TIME FOR SEVERAL POINTS WITHIN A CLOSED SQUARE WITH A WELL AT THE CENTER

DIMENSIONLESS TIME t_{Da}	DIMENSIONLESS PRESSURE DROP								
	$x_D=0.000$ $y_D=0.000$	$x_D=0.250$ $y_D=0.000$	$x_D=0.250$ $y_D=0.250$	$x_D=0.500$ $y_D=0.000$	$x_D=0.500$ $y_D=0.250$	$x_D=0.500$ $y_D=0.500$	$x_D=0.750$ $y_D=0.000$	$x_D=0.750$ $y_D=0.250$	$x_D=0.750$ $y_D=0.500$
0.0010	4.5516	0.0021	0.0000	0.0000	0.0000	0.0000	0.0000	0.0000	0.0000
0.0015	4.7543	0.0109	0.0004	0.0000	0.0000	0.0000	0.0000	0.0000	0.0000
0.0020	4.8981	0.0261	0.0021	0.0000	0.0000	0.0000	0.0000	0.0000	0.0000
0.0025	5.0097	0.0456	0.0056	0.0001	0.0000	0.0000	0.0000	0.0000	0.0000
0.0030	5.1009	0.0675	0.0109	0.0004	0.0001	0.0000	0.0000	0.0000	0.0000
0.0040	5.2447	0.1141	0.0261	0.0021	0.0007	0.0000	0.0000	0.0000	0.0000
0.0050	5.3563	0.1607	0.0456	0.0056	0.0021	0.0001	0.0001	0.0001	0.0000
0.0060	5.4474	0.2053	0.0675	0.0109	0.0047	0.0004	0.0004	0.0002	0.0001
0.0070	5.5245	0.2475	0.0906	0.0178	0.0085	0.0011	0.0011	0.0006	0.0003
0.0080	5.5913	0.2871	0.1141	0.0261	0.0135	0.0021	0.0021	0.0012	0.0007
0.0090	5.6502	0.3243	0.1376	0.0354	0.0194	0.0036	0.0036	0.0021	0.0013
0.0100	5.7029	0.3592	0.1607	0.0456	0.0261	0.0056	0.0056	0.0034	0.0021
0.0150	5.9056	0.5063	0.2676	0.1023	0.0675	0.0218	0.0218	0.0154	0.0109
0.0200	6.0494	0.6211	0.3592	0.1607	0.1142	0.0456	0.0456	0.0350	0.0266
0.0250	6.1610	0.7147	0.4379	0.2164	0.1609	0.0735	0.0735	0.0597	0.0474
0.0300	6.2522	0.7939	0.5065	0.2685	0.2061	0.1032	0.1032	0.0876	0.0716
0.0400	6.3965	0.9232	0.6224	0.3628	0.2906	0.1650	0.1650	0.1445	0.1263
0.0500	6.5099	1.0279	0.7192	0.4470	0.3685	0.2276	0.2276	0.2175	0.1854
0.0600	6.6050	1.1178	0.8041	0.5242	0.4415	0.2904	0.2904	0.2772	0.2466
0.0700	6.6888	1.1983	0.8815	0.5968	0.5112	0.3532	0.3532	0.3418	0.3086
0.0800	6.7654	1.2728	0.9539	0.6661	0.5786	0.4160	0.4160	0.4061	0.3711
0.0900	6.8374	1.3434	1.0231	0.7334	0.6446	0.4788	0.4788	0.4700	0.4338
0.1000	6.9063	1.4114	1.0902	0.7992	0.7095	0.5417	0.5417	0.5336	0.4965
0.1500	7.2311	1.7347	1.4119	1.1186	1.0274	0.8556	0.8556	0.8492	0.8106
0.2000	7.5468	2.0501	1.7271	1.4335	1.3421	1.1700	1.1700	1.1636	1.1248
0.2500	7.8611	2.3644	2.0414	1.7478	1.6563	1.4841	1.4841	1.4774	1.4390
0.3000	8.1753	2.6786	2.3556	2.0620	1.9705	1.7983	1.7983	1.7919	1.7531
0.4000	8.8036	3.3069	2.9839	2.6903	2.5988	2.4266	2.4266	2.4202	2.3814
0.5000	9.4320	3.9352	3.6122	3.3186	3.2271	3.0549	3.0549	3.0486	3.0098
0.6000	10.0603	4.5636	4.2406	3.9469	3.8555	3.6833	3.6833	3.6769	3.6381
0.7000	10.6886	5.1919	4.8689	4.5752	4.4838	4.3116	4.3116	4.3052	4.2664
0.8000	11.3169	5.8202	5.4972	5.2036	5.1121	4.9399	4.9399	4.9335	4.8947
0.9000	11.9452	6.4485	6.1255	5.8319	5.7404	5.5682	5.5682	5.5618	5.5230
1.0000	12.5735	7.0768	6.7538	6.4602	6.3687	6.1965	6.1965	6.1902	6.1513
2.0000	18.8567	13.3600	13.0370	12.7433	12.6515	12.4797	12.4797	12.4733	12.4345
4.0000	31.4230	25.9263	25.6033	25.3097	25.2182	25.0460	25.0460	25.0397	25.0009
8.0000	56.5557	51.0590	50.7360	50.4423	50.3509	50.1787	50.1787	50.1723	50.1335
10.0000	69.1220	63.6253	63.3023	63.0087	62.9172	62.7450	62.7450	62.7386	62.6999

DIMENSIONLESS TIME t_{Da}	DIMENSIONLESS PRESSURE DROP								
	$x_D=0.750$ $y_D=0.500$	$x_D=0.750$ $y_D=0.750$	$x_D=0.875$ $y_D=0.000$	$x_D=0.875$ $y_D=0.500$	$x_D=1.000$ $y_D=0.000$	$x_D=1.000$ $y_D=0.250$	$x_D=1.000$ $y_D=0.500$	$x_D=1.000$ $y_D=0.750$	$x_D=1.000$ $y_D=1.000$
0.0010	0.0000	0.0000	0.0000	0.0000	0.0000	0.0000	0.0000	0.0000	0.0000
0.0015	0.0000	0.0000	0.0000	0.0000	0.0000	0.0000	0.0000	0.0000	0.0000
0.0020	0.0000	0.0000	0.0000	0.0000	0.0000	0.0000	0.0000	0.0000	0.0000
0.0025	0.0000	0.0000	0.0000	0.0000	0.0000	0.0000	0.0000	0.0000	0.0000
0.0030	0.0000	0.0000	0.0000	0.0000	0.0000	0.0000	0.0000	0.0000	0.0000
0.0040	0.0000	0.0000	0.0000	0.0000	0.0000	0.0000	0.0000	0.0000	0.0000
0.0050	0.0000	0.0000	0.0000	0.0000	0.0000	0.0000	0.0000	0.0000	0.0000
0.0060	0.0000	0.0000	0.0000	0.0000	0.0000	0.0000	0.0000	0.0000	0.0000
0.0070	0.0000	0.0000	0.0001	0.0000	0.0000	0.0000	0.0000	0.0000	0.0000
0.0080	0.0001	0.0000	0.0002	0.0000	0.0000	0.0000	0.0000	0.0000	0.0000
0.0090	0.0003	0.0000	0.0004	0.0001	0.0001	0.0001	0.0001	0.0000	0.0000
0.0100	0.0005	0.0001	0.0006	0.0001	0.0003	0.0002	0.0000	0.0000	0.0000
0.0150	0.0040	0.0008	0.0055	0.0016	0.0031	0.0023	0.0009	0.0002	0.0001
0.0200	0.0121	0.0036	0.0164	0.0060	0.0111	0.0087	0.0042	0.0014	0.0005
0.0250	0.0245	0.0091	0.0329	0.0143	0.0249	0.0203	0.0117	0.0045	0.0023
0.0300	0.0404	0.0177	0.0539	0.0264	0.0436	0.0365	0.0219	0.0102	0.0062
0.0400	0.0805	0.0437	0.1050	0.0600	0.0913	0.0793	0.0532	0.0307	0.0223
0.0500	0.1281	0.0800	0.1628	0.1030	0.1469	0.1308	0.0947	0.0623	0.0498
0.0600	0.1807	0.1241	0.2237	0.1525	0.2065	0.1871	0.1431	0.1029	0.0872
0.0700	0.2366	0.1740	0.2859	0.2064	0.2678	0.2460	0.1962	0.1521	0.1321
0.0800	0.2948	0.2279	0.3486	0.2632	0.3299	0.3064	0.2525	0.2023	0.1826
0.0900	0.3546	0.2846	0.4114	0.3219	0.3925	0.3677	0.3109	0.2579	0.2369
0.1000	0.4153	0.3433	0.4744	0.3820	0.4551	0.4296	0.3708	0.3157	0.2939
0.1500	0.7257	0.6500	0.7888	0.6913	0.7692	0.7421	0.6797	0.6209	0.5976
0.2000	1.0393	0.9632	1.1030	1.0047	1.0834	1.0561	0.9931	0.9338	0.9103
0.2500	1.3534	1.2772	1.4172	1.3188	1.3975	1.3702	1.3071	1.2478	1.2243
0.3000	1.6676	1.5913	1.7313	1.6330	1.7117	1.6843	1.6213	1.5620	1.5384
0.4000	2.2959	2.2196	2.3597	2.2613	2.3400	2.3127	2.2496	2.1903	2.1667
0.5000	2.9242	2.8479	2.9880	2.8896	2.9683	2.9410	2.8779	2.8186	2.7950
0.6000	3.5525	3.4763	3.6163	3.5179	3.5966	3.5693	3.5062	3.4469	3.4233
0.7000	4.1808	4.1046	4.2446	4.1462	4.2249	4.1976	4.1346	4.0752	4.0517
0.8000	4.8092	4.7329	4.8729	4.7745	4.8533	4.8259	4.7629	4.7036	4.6800
0.9000	5.4375	5.3612	5.5012	5.4029	5.4816	5.4542	5.3912	5.3319	5.3083
1.0000	6.0658	5.9895	6.1296	6.0312	6.1099	6.0826	6.0195	5.9602	5.9366
2.0000	12.3490	12.2727	12.4127	12.3144	12.3930	12.3657	12.3027	12.2434	12.2198
4.0000	24.9153	24.8391	24.9791	24.8807	24.9594	24.9321	24.8690	24.8097	24.7861
8.0000	50.0480	49.9717	50.1117	50.0134	50.0921	50.0647	50.0017	49.9424	49.9188
10.0000	62.6143	62.5381	62.6781	62.5797	62.6584	62.6311	62.5680	62.5087	62.4851

due of
1 point
r only
all t_{DA} .

Grid point pressures become essentially independent of \sqrt{A}/r_w for values of $(t_{DA}A/r_w^2)$ greater than 20. This corresponds to $t_{DA} > 5 \times 10^{-6}$ for the value of \sqrt{A}/r_w used here. Results can be extended to smaller values of \sqrt{A}/r_w by subtracting the pressure contributions of the closest image wells and replacing them by more accurate cylindrical source pressure contributions.

For convenience, the dimensionless space variables (x_D, y_D) used in Table 1 are defined as fractions of the total length of the side of the square. The origin is taken at the well (Fig. 1). That is,

$$x_D = x/L = 2x/\sqrt{A}, \dots \dots \dots (13)$$

$$y_D = y/L = 2y/\sqrt{A}, \dots \dots \dots (14)$$

where $L = \frac{1}{2}\sqrt{A}$. Thus, the ratio $r_w/L = 0.001$.

Fig. 2 is a plot of the dimensionless pressure vs dimensionless time for some of the points included in Table 1. The figure shows that at sufficiently long times the system exhibits pseudo-steady-state behavior; i.e., the dimensionless pressure becomes a linear function of dimensionless time. Thus, pressures may be found at times greater than those in the table by linear extrapolation.

The time at which various grid points reach the pseudo-steady-state condition varies considerably with the grid location. Surprisingly, some of the grid points distant from the well reach pseudo-steady state long before the well point does. For example, compare grid locations (0.5, 0.5), (0.25, 0.25) and the well point (0.001, 0). The information in Table 1 can also be displayed on a log-log plot to advantage (Fig. 3). Expanded plots of this type are convenient for interpolation during the early transient period.

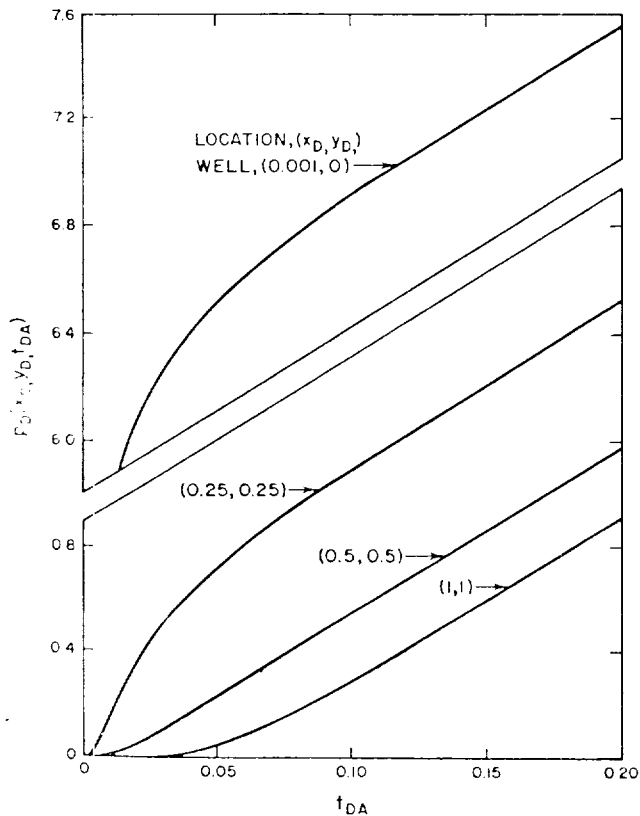


Fig. 2—Dimensionless pressure $p_D(x_D, y_D, t_{DA})$ as function of dimensionless time t_{DA} for a well in center of a closed square (constant production rate and $\sqrt{A}/r_w = 2,000$).

The pseudo steady-state condition discussed in connection with Fig. 2 can be illustrated in another way. Because pressures at every location in the square change at the same rate during fully developed pseudo-steady flow, it is possible to plot a generalized isobaric map for this period (Fig. 4). The isobars shown on Fig. 4 are identified as the difference between the pressure at the location shown and that at point (1, 1). This type of plot has the advantage that the \sqrt{A}/r_w effect is eliminated. The isobars of Fig. 4 may be converted to appropriate dimensionless pressures at any given time by noting the corresponding dimensionless pressures from Table 1.

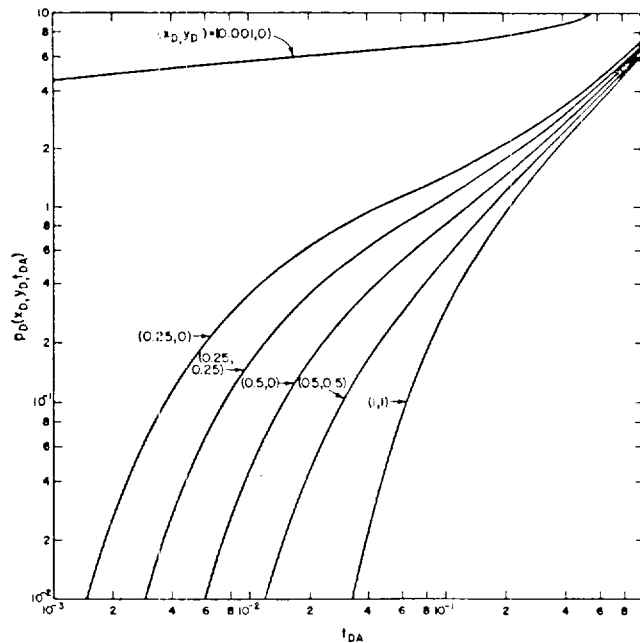


Fig. 3—Dimensionless pressure vs dimensionless time, well in center of a closed square.

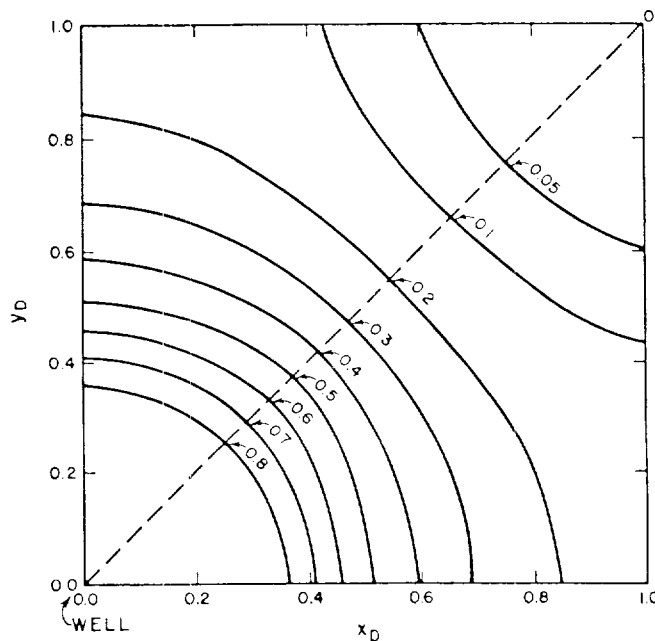


Fig. 4—Isopotentials for pseudo-steady-state depletion, well in center of closed square (isopotentials are $[p_i(x_D, y_D, t_{DA}) - p_D(1, 1, t_i)]$ for $t_{DA} \geq 0.1$).

0.000
0.000
0.000
0.000
0.000
0.000
0.000
0.000
0.000
0.000
0.000
0.001
0.005
0.023
0.062
0.223
0.498
0.872
1.21
1.626
2.069
2.519
2.976
3.43
3.884
4.367
4.850
5.333
5.817
6.300
6.783
7.266
7.750
8.233
8.717
9.200
9.683
10.166
10.650

TABLE 2—MATTHEWS-BRONS-HAZELBROEK DIMENSIONLESS PRESSURE LOSS FOR VARIOUS RECTANGULAR SYSTEMS

DIMENSIONLESS TIME t_{DA}	MAH DIMENSIONLESS PRESSURE DROP							
								
0.0010	0.0126	0.0126	0.0126	0.0126	0.0126	0.0126	0.0126	0.0126
0.0015	0.0185	0.0185	0.0185	0.0185	0.0185	0.0185	0.0185	0.0185
0.0020	0.0251	0.0251	0.0251	0.0251	0.0251	0.0251	0.0251	0.0251
0.0025	0.0314	0.0314	0.0314	0.0314	0.0314	0.0314	0.0314	0.0314
0.0030	0.0377	0.0377	0.0377	0.0377	0.0377	0.0377	0.0377	0.0377
0.0040	0.0503	0.0503	0.0503	0.0503	0.0503	0.0503	0.0503	0.0503
0.0050	0.0628	0.0628	0.0628	0.0628	0.0628	0.0628	0.0628	0.0628
0.0060	0.0754	0.0754	0.0754	0.0754	0.0754	0.0754	0.0754	0.0754
0.0070	0.0880	0.0880	0.0880	0.0880	0.0880	0.0880	0.0880	0.0880
0.0080	0.1005	0.1005	0.1005	0.1005	0.1005	0.1005	0.1005	0.1005
0.0090	0.1131	0.1131	0.1131	0.1131	0.1131	0.1131	0.1131	0.1131
0.0100	0.1257	0.1257	0.1257	0.1257	0.1257	0.1257	0.1257	0.1257
0.0150	0.1885	0.1854	0.1823	-0.0162	0.1884	0.1849	0.1884	0.1849
0.0200	0.2513	0.2402	0.2287	-0.0700	0.2508	0.1761	0.2505	0.1598
0.0250	0.3141	0.2892	0.2630	-0.1181	0.3119	0.1674	0.3107	0.1663
0.0300	0.3769	0.3333	0.2864	-0.1584	0.3708	0.1723	0.3676	0.1683
0.0400	0.5016	0.4108	0.3087	-0.2166	0.4874	0.1812	0.4684	0.1657
0.0500	0.6237	0.4791	0.3099	-0.2512	0.5745	0.1955	0.5511	0.1593
0.0600	0.7415	0.5413	0.3002	-0.2694	0.6647	0.2149	0.6147	0.1513
0.0700	0.8537	0.5991	0.2856	-0.2766	0.7471	0.2290	0.6883	0.1428
0.0800	0.9597	0.6531	0.2700	-0.2765	0.8217	0.2450	0.7085	0.1386
0.0900	1.0592	0.7035	0.2553	-0.2716	0.8817	0.3147	0.7394	0.1294
0.1000	1.1524	0.7516	0.2427	-0.2633	0.9381	0.3541	0.7642	0.1194
0.1500	1.5364	0.9583	0.2226	-0.1951	1.2524	0.5884	0.8241	0.0954
0.2000	1.8212	1.1314	0.2037	-0.1027	1.4997	0.8176	0.8474	0.0873
0.2500	2.0439	1.2854	0.1842	0.0025	1.7044	1.0104	0.8629	0.0823
0.3000	2.2262	1.4257	0.1665	0.1129	1.8830	1.1841	0.8829	0.1087
0.4000	2.5139	1.6720	0.1490	0.3309	2.1678	1.4674	0.9447	0.1687
0.5000	2.7370	1.8797	0.1311	0.5268	2.3995	1.6864	1.0299	0.2537
0.6000	2.9193	2.0563	0.1128	0.6994	2.5728	1.8722	1.1280	0.3518
0.7000	3.0735	2.2053	0.1027	0.8499	2.7249	2.0243	1.2307	0.4545
0.8000	3.2070	2.3411	0.0987	0.9821	2.8675	2.1594	1.3329	0.5567
0.9000	3.3249	2.4586	0.0919	1.0994	2.9742	2.2776	1.4315	0.6557
1.0000	3.4302	2.5638	0.9070	1.2045	3.0836	2.3830	1.5252	0.7449
2.0000	4.1234	3.2569	2.2000	1.8976	3.7748	3.0742	2.2002	1.4234
4.0000	4.8166	3.9501	2.8933	2.5906	4.4701	3.7695	2.8932	2.1171
6.0000	5.5099	4.6435	3.5867	3.2842	5.1633	4.4627	3.5864	2.8103
10.0000	5.7331	4.8667	3.8098	3.5073	5.3885	4.6859	3.8098	3.0335

DIMENSIONLESS TIME t_{DA}	MAH DIMENSIONLESS PRESSURE DROP							
								
0.0010	0.0125	0.0125	0.0125	0.0125	0.0125	0.0125	0.0125	0.0125
0.0015	0.0179	0.0188	0.0179	0.0188	0.0188	0.0188	0.0188	0.0188
0.0020	0.0209	0.0251	0.0209	0.0251	0.0251	0.0251	0.0251	0.0251
0.0025	0.0203	0.0314	0.0203	0.0314	0.0314	0.0314	0.0314	0.0314
0.0030	0.0160	0.0377	0.0155	0.0377	0.0377	0.0377	0.0377	0.0377
0.0040	-0.0019	0.0503	-0.0027	0.0503	0.0503	0.0503	0.0503	0.0503
0.0050	-0.0284	0.0628	-0.0295	0.0628	0.0628	0.0628	0.0628	0.0628
0.0060	-0.0596	0.0745	-0.0612	0.0745	0.0745	0.0745	0.0745	0.0745
0.0070	-0.0932	0.0858	-0.0951	0.0858	0.0858	0.0858	0.0858	0.0858
0.0080	-0.1277	0.0962	-0.1296	0.1004	0.0962	0.1004	0.0962	0.1004
0.0090	-0.1620	0.105	-0.1644	0.1129	0.0962	0.1129	0.0962	0.1129
0.0100	-0.1957	0.1144	-0.1983	0.1251	0.0962	0.1251	0.0962	0.1251
0.0150	-0.3465	0.1445	-0.3502	0.1873	-0.0142	0.1823	-0.0142	0.1714
0.0200	-0.4670	0.1589	-0.4718	0.2291	-0.0701	0.2291	-0.0701	0.2015
0.0250	-0.5615	0.1641	-0.5695	0.2643	-0.1146	0.2643	-0.1146	0.2183
0.0300	-0.6357	0.1633	-0.6507	0.2897	-0.1620	0.2897	-0.1620	0.2200
0.0400	-0.7395	0.1492	-0.7839	0.3197	-0.2211	0.3194	-0.2235	0.2075
0.0500	-0.8012	0.1274	-0.8965	0.3332	-0.2642	0.3315	-0.2642	0.1820
0.0600	-0.8339	0.0862	-0.9969	0.3385	-0.2957	0.3335	-0.3013	0.1516
0.0700	-0.8457	0.0437	-1.0949	0.3399	-0.3156	0.3200	-0.3278	0.1203
0.0800	-0.8422	-0.0028	-1.1859	0.3401	-0.3291	0.3194	-0.3350	0.0899
0.0900	-0.8277	-0.0512	-1.2723	0.3403	-0.3375	0.3072	-0.3427	0.0613
0.1000	-0.8038	-0.1004	-1.3542	0.3412	-0.3421	0.2945	-0.3492	0.0351
0.1500	-0.4223	-0.3322	-1.7021	0.3663	-0.3257	0.3426	-0.3128	-0.0540
0.2000	-0.4130	-0.5189	-2.0613	0.4269	-0.2661	0.4048	-0.2649	-0.0935
0.2500	-0.2196	-0.6581	-2.1507	0.5120	-0.1811	0.4694	-0.1792	-0.0845
0.3000	-0.0479	-0.7555	-2.2854	0.6102	-0.0829	0.5344	-0.0932	-0.0477
0.4000	0.2343	-0.8547	-2.3344	0.8152	0.1220	0.6749	-1.1758	0.0773
0.5000	0.4567	-0.8671	-2.4768	1.0075	0.3163	0.8075	-1.3641	0.2264
0.6000	0.6389	-0.8284	-2.4564	1.1783	0.4852	0.8814	-1.5103	0.3754
0.7000	0.7931	-0.7620	-2.4011	1.3282	0.6351	0.9129	-1.6094	0.5143
0.8000	0.9267	-0.6820	-2.3278	1.4602	0.7670	0.9775	-1.6744	0.6409
0.9000	1.0444	-0.5969	-2.2465	1.5774	0.8843	1.0145	-1.7114	0.7555
1.0000	1.1497	-0.5115	-2.1640	1.6825	0.9890	1.0393	-1.7270	0.8588
2.0000	1.8430	-0.1507	-1.4056	2.3755	1.6824	-0.1725	-1.4296	1.5534
4.0000	2.5363	0.8436	-0.8129	3.0688	2.3757	-0.0756	-0.7725	2.2484
6.0000	3.2295	1.5370	-0.1195	3.7623	3.0681	-0.0173	-0.0794	2.9381
10.0000	3.4527	1.7601	0.1036	3.9854	3.2902	0.0486	0.1434	3.1615

Pressure Distributions in Rectangular Shapes

Although the calculation technique used to produce pressure distributions for the square also can be used to obtain tabular pressure data for other rectangular shapes, it does not appear worthwhile to do so. It will be shown that the results for the square shape may easily be superposed to produce the same result. However, the Matthews-Brons-Hazebrook pressure buildup correction function p_{DMBH} , previously cited as Eq. 10, was computed for a number of rectangular shapes (Table 2). Although this information is already available in graphical form in Ref. 6, it often is useful to have tabulations of such data. This table also may be generated from the solutions for the square shape by superposition (simple addition of columns of numbers).

One application for the Matthews-Brons-Hazebrook pressure function is determination of shape factors for the pseudo-steady-state flow condition. Brons and Miller⁷ showed that it is possible to assign shape factors C_A for the pseudo-steady-state flow condition for a variety of drainage shapes. Later, Dietz⁸ tabulated shape factors for the Matthews-Brons-Hazebrook shapes as determined from their graphical data. Table 2 may be used to obtain more accurate values of the shape factors. For the pseudo-steady-state condition Eq. 10 may be written

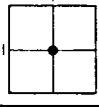
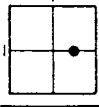
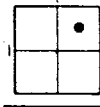
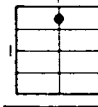
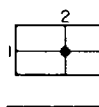
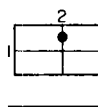
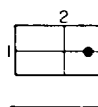
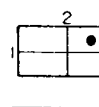
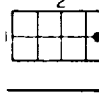
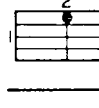
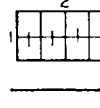
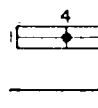
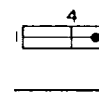
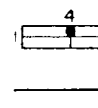
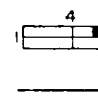
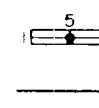
$$p_{DMBH} = \ln(C_A t_{DA}) \quad (15)$$

Thus, the natural logarithm of the shape factor may be determined from tabulated values of p_{DMBH} at dimensionless times t_{DA} of unity, if pseudo-steady-state has been attained at that time. Otherwise, an extrapolation back to $t_{DA} = 1.0$ is necessary. Table 3 presents some shape factors determined in this fashion and compares results with those of Dietz. Shape factors for other systems are available in Ref. 9, and others may be generated by superposition of the square shape solutions presented in Table 1.

It can be seen from Eqs. 10 and 11 that the p_{DMBH} values given in Table 2 may be used to generate the dimensionless pressure drop at the well for each shape tabulated. The same result may be obtained by using the information in Table 1 and superposition. For example, suppose the pressure behavior is required for a well in the center of a rectangle with sides in the ratio of 2:1. The behavior of this system could be calculated by using Eq. 11 for an infinite array of wells (Fig. 1), but with the distance between wells in the y direction equal to half the distance between wells in the x direction. This particular well array will result if a second array of wells like that shown in Fig. 1 is superimposed on the grid shown in Fig. 1 such that the origin well of the second array is located at $x_D = 0, y_D = 1.0$. This is equivalent to overlaying a square system with a well in the center with another one, but with the second well at point (0, 1.0). The area of the 2:1 rectangle formed A' is half the area of the initial square A . The pressure drop at any point within the 2:1 rectangle is simply the sum of the pressure drops caused by each of the two square systems at the common location.

Fig. 5 illustrates the superposition of the two square arrays of wells described previously. The open circles indicate locations of wells in the initial square array, while the solid circles indicate locations of the superimposed square array. It is clear that the new unit of symmetry is a 2:1 rectangle with a well at the center. Suppose we wish to find the dimensionless pressure at the point (x, y) shown on Fig. 5. This point is located at (0.5, 0) in the original square grid, and at (1, 0.5)—which is the same as (0.5, 1) by symmetry—in the superimposed grid. The dimensionless pressure drops from the (0.5, 0) and (1, 0.5) columns of Table 1 are added to generate the dimensionless pressure drop for the 2:1 rectangle at the location shown. However, note that the dimensionless times t_{DA} change because the drainage area A' of the rectangle is half the original drain

TABLE 3—PSEUDO-STEADY-STATE SHAPE FACTORS FOR VARIOUS RECTANGULAR SYSTEMS

								
$\ln C_A$ (this paper)	3.4302	2.5638	1.5070	1.2045	3.0836	2.3830	1.5072	0.7309
(Dietz)	3.43	2.56	1.52	1.22	3.12	2.38	1.58	0.73
C_A (this paper)	30.8828	12.9851	4.5132	3.3351	21.8369	10.8374	4.5141	2.0769
(Dietz)	30.9	12.9	4.57	3.39	22.6	10.8	4.86	2.07
for $t_{DA} >$	0.3	0.7	0.6	0.7	0.3	0.4	1.5	1.7
								
$\ln C_A$ (this paper)	-0.5425	1.1497	-2.1990	1.6825	-1.4620	0.9894	-2.1588	0.8589
(Dietz)	-0.50	1.14	-2.20	1.68	-1.46	1.00	-2.16	0.86
C_A (this paper)	0.5813	3.1573	0.1109	5.3790	0.2318	2.6896	0.1155	2.3606
(Dietz)	0.607	3.13	0.111	5.38	0.232	2.72	0.115	2.36
for $t_{DA} >$	2.0	0.4	3.0	0.8	4.0	0.8	4.0	1.0

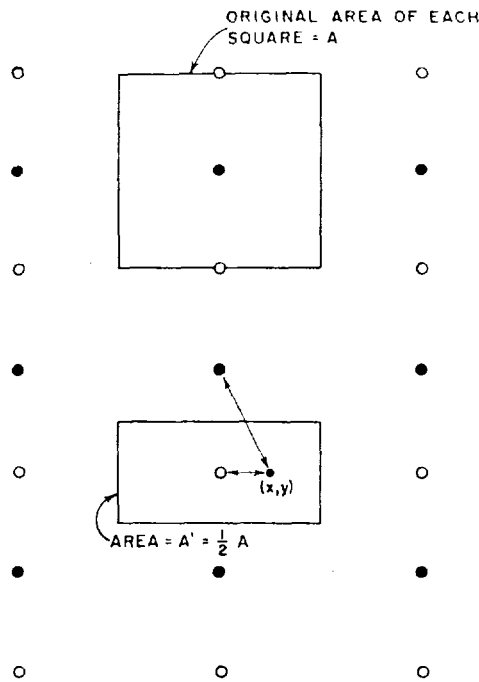


Fig. 5—Superposition of two square arrays to form a 2:1 rectangle.

age area of each square A . Thus, the corresponding dimensionless times are twice those in Table 1. Steps in this calculation are shown in Table 4.

If the pressure at the well in the rectangle is required, pressures from Table 1 for the well location are added to those for point $(1, 0)$ —which is the same as $(0, 1)$ by symmetry. Again, the dimensionless time for the rectangle will

be twice that for the squares because of the reduction in the drainage area caused by superposition. The ratio $\sqrt{A'}/r_w$ will now be $\sqrt{1/2} A/r_w$, or $1,000 \sqrt{2}$. If the dimensionless pressure at the well for a 2:1 rectangle with $\sqrt{A'}/r_w = 2,000$ is desired, then the term $\ln(2,000/[1,000\sqrt{2}])$ must be added to each entry of Column 6 in Table 4, as is apparent from Eq. 12. Note that conventional dimensionless time t_D based on the well radius would be the same for both the square and rectangle since the well radius does not change.

It should be clear that it is possible to generate an entire table of pressure-time-location data for the 2:1 rectangle from the results for the square given in Table 1. One interesting feature of the superposition becomes evident here. Consider Fig. 5 again. If another infinite array of 2:1 rectangles were superimposed over this grid such that the origin well falls at point $x_D = 1.0, y_D = 0$ in the existing 2:1 rectangle, the well array would return to the original square array but with one-quarter the original drainage area; dimensionless times t_{DA} would now be four times the original values for the square array in Table 1. In addition, the ratio of the side length of the square to the well radius would change to $\sqrt{1/4} A/r_w$ or 1,000. This is an alternate way to extrapolate times or to change the \sqrt{A}/r_w ratio.

A large variety of patterns can be generated by the technique just described by varying the location and number of superposed wells. For example, another 2:1 rectangular array could be added to that of Fig. 5 such that the wells would fall halfway, vertically, between the existing wells. This would generate a 4:1 rectangle with the well at the center. The same result also could be achieved by adding four square arrays together.

Superposition of square arrays also can be used to move the well off-center in a square or rectangular shape, or to

TABLE 4—CALCULATION OF $p_D(x_D, y_D, t_{DA})$ FOR 2:1 RECTANGLE

(1) t_{DA}	$p_D(x_D, y_D, t_{DA})$ for Square at Locations of				$p_D(x_D, y_D, t_{DA})$ for 2:1 Rectangle at		
	(2) r_w	(3) (0.5, 0)	(4) (1, 0)	(5) (1, 0.5)	(6) r_w (2)+(4)	(7) (0.5, 0) (3)+(5)	(8) t_{DA} (2)(1)
	*				**	***	
.0010	4.5516	.0000	.0000	.0000	4.5516	.0000	.0020
.0015	4.7543	.0000	.0000	.0000	4.7543	.0000	.0030
.0020	4.8981	.0000	.0000	.0000	4.8981	.0000	.0040
.0025	5.0097	.0001	.0000	.0000	5.0097	.0001	.0050
.0030	5.1009	.0004	.0000	.0000	5.1009	.0004	.0060
.0040	5.2447	.0021	.0000	.0000	5.2447	.0021	.0080
.0050	5.3563	.0056	.0000	.0000	5.3563	.0056	.0100
.0060	5.4474	.0109	.0000	.0000	5.4474	.0109	.0120
.0070	5.5245	.0178	.0000	.0000	5.5245	.0178	.0140
.0080	5.5913	.0261	.0000	.0000	5.5913	.0261	.0160
.0090	5.6502	.0354	.0001	.0000	5.6503	.0354	.0180
.0100	5.7029	.0456	.0003	.0000	5.7032	.0456	.0200
.0150	5.9056	.1023	.0031	.0009	5.9087	.1032	.0300
.0200	6.0494	.1607	.0111	.0042	6.0605	.1649	.0400
.0250	6.1610	.2164	.0249	.0112	6.1859	.2276	.0500
.0300	6.2522	.2685	.0436	.0219	6.2958	.2904	.0600
.0400	6.3965	.3628	.0913	.0532	6.4878	.4160	.0800
.0500	6.5099	.4470	.1469	.0947	6.6568	.5417	.1000
.0600	6.6050	.5242	.2065	.1431	6.8115	.6673	.1200
.0700	6.6888	.5968	.2678	.1962	6.9566	.7930	.1400
.0800	6.7654	.6661	.3299	.2525	7.0953	.9186	.1600
.0900	6.8374	.7334	.3925	.3109	7.2299	1.0443	.1800
.1000	6.9063	.7992	.4551	.3708	7.3614	1.1700	.2000

* $\sqrt{A}/r_w = 2,000$.

** $\sqrt{A'}/r_w = \sqrt{\frac{1}{2} A}/r_w = 1,000 \sqrt{2}$.

*** Dimensionless coordinates are fractions of half length and width of 2:1 rectangle, origin at well in center.

geometric shapes containing more than one well. The wells can be placed in almost any position within almost any rectangular shape. Only the basic data of the pressure distribution for the square array given in Table 1 are needed to do this. One convenient way to make these superpositions is to use a series of transparent sheets, each containing the well array for a square with the well at the center. These sheets can be laid one over another until the desired well array is obtained.*

The square array also may be used with superposition to generate constant-pressure outer boundary conditions. Fig. 6 illustrates the well array needed to generate this case for a square shape. A second square grid of injection wells falls midway between the wells of the original grid. This generates a constant pressure boundary as shown by the solid lines of Fig. 6. The injection-production pattern shown in Fig. 6 is the well known developed five-spot unit mobility ratio case discussed thoroughly by Muskat¹⁰ and many others. Muskat pointed out that the result for such injection-production cases could be interpreted as the constant-pressure boundary condition case. However, the method outlined in this study has a number of practical features that indicate that even cases like those considered in Fig. 6 are not trivial. The information in this paper may be used to find the unsteady portion of the pressure history as well as the pseudo-steady-state or true steady-state portions. Such information has not been available previously.

A useful application of dimensionless pressure functions is the generation of pressure functions and buildup curves for unusual cases not currently available. For example, a well adjacent to an oil-water contact but surrounded by producing wells on three other sides might behave like a well in a geometric shape with three sides closed to flow, but with the fourth side maintained at constant pressure. Superposition of injection and production arrays can produce such mixtures of outer boundary conditions. For ex-

*An Appendix outlining a simple method for making superpositions without using transparent well arrays was presented in the original preprint of the paper.

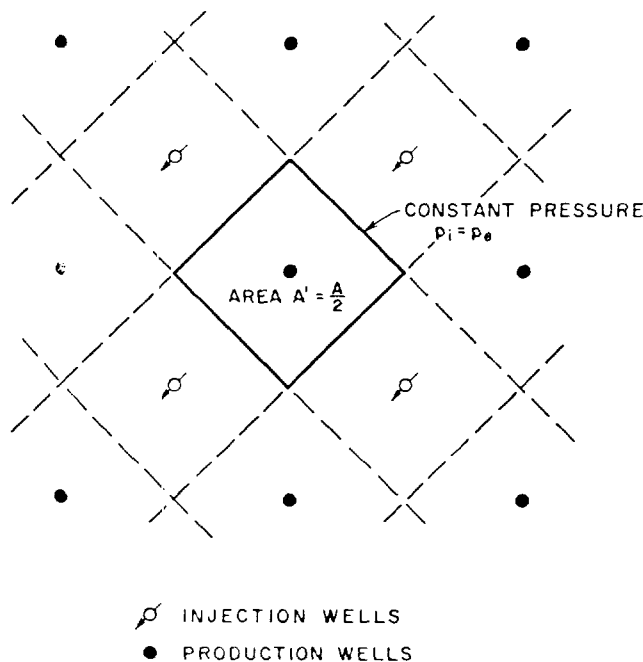


Fig. 6—Superposition pattern for constant pressure boundary condition (square shape).

ample, superposition of an array of production wells located in the center of one of the two squares composing a 2:1 rectangle and another array of injection wells located in the opposite square of the 2:1 rectangle will generate the behavior of a well located in the center of a square with three sides closed and with one side at constant pressure. Fig. 7 presents the Miller-Dyes-Hutchinson¹² pressure buildup functions p_{pDMDH} for several rectangular shapes.** Note that any shape that has a constant pressure condition over any portion of the outer boundary will always reach a steady state, and will build up to constant pressure p_s . On the other hand, any shape which has a completely closed outer boundary will build up to the mean pressure \bar{p} . This can lead to confusion. Using Fig. 7 for cases involving constant pressure over a portion of the outer boundary will yield extrapolated estimates of the initial pressure $p_i = p_s$. This is the same approach as used by Miller, Dyes and Hutchinson.¹² On the other hand, Dietz⁹ also discussed extrapolation of buildup pressures for the circular shape with constant pressure over the outer boundary. Dietz' method yields the mean pressure \bar{p} within the circular shape, rather than $p_i = p_s$. For any shape, the difference between \bar{p} and p_i will be a constant during pseudo-steady state. For the circular reservoir case,

$$p_i - \bar{p} = \frac{q\mu}{4\pi kh} \dots \dots \dots (16)$$

Thus, the difference in pressure for the circular shape is equal to the slope of the straight-line portion of the buildup test. Similar constants for other geometric shapes are not available. Such constants could be developed readily by computing the volumetric mean pressure \bar{p} for any specific shape.

Fig. 7 has several interesting features. A comparison of the second and fourth curves from the top indicates that a mixed outer boundary condition can cause a bend in the pressure buildup curve similar to faulting or heterogeneity—even for a very regular shape such as a square with a centered well. The fifth curve shows a rather extreme case of this sort for a 2:1 rectangle. It is clear that it might be extremely difficult to identify the proper straight line for this case. Note also that there is a time displacement of the buildup curve for any given shape (as well as a shape change of the curve) as the outer boundary condition changes.

**Full page copies of Fig. 7 with a complete grid are available from the authors on request.

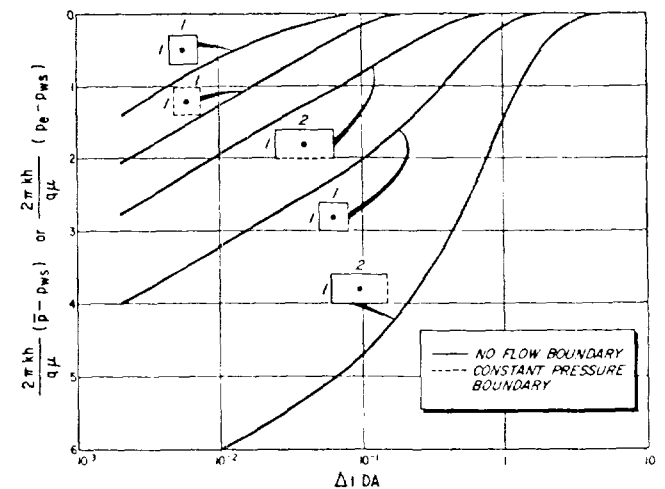


Fig. 7—Miller-Dyes-Hutchinson pressure buildup curves for rectangular shapes.

Fig. 8 shows several injection-production well patterns that result in square shapes having a well at the center and a combination of no-flow and constant pressure boundaries. All of these patterns can be produced using the information in Table 1. Note that the wells located on straight boundaries have their rates reduced by a factor of $1/2$, and the wells located on the corners have their rates reduced by a factor of $1/4$. However, after superposition, the sums of the dimensionless pressure drops for the wells with fractional rates add up to the dimensionless pressure drop for a well with the full rate. For example, in the last case shown in Fig. 8, $p_D(r_w, t_{DA}) = p_D(0, 0, 1/4 t_{DA}) + p_D(1, 1, 1/4 t_{DA}) - 2p_D(1, 0, 1/4 t_{DA})$ and $\sqrt{A}/r_w = 1,000$. The configurations given in Fig. 8 are not necessarily the only ones that will give the desired result. For instance, the behavior of a square with constant pressure boundaries on all four sides may be calculated from $p_D(r_w, t_{DA}) = p_D(0, 0, 1/2 t_{DA}) - p_D(1, 1, 1/2 t_{DA})$ as well as from the expression above. In this case, $\sqrt{A}/r_w = 1,000\sqrt{2}$. Well locations and shapes other than those shown in Fig. 8 also may be generated.

The mode of superposition can be varied considerably from that already illustrated. For example, it is not necessary that injection and production rates be constant or be the same, nor even that injection and production start at the same time. Since superposition has been used to add together the effects of the two types of wells, it is clear that the pressure drop caused by each type of well is independent of the behavior of the other. Furthermore, the generalization can be made that it is not necessary that the drainage area of two or more square arrays be the same.

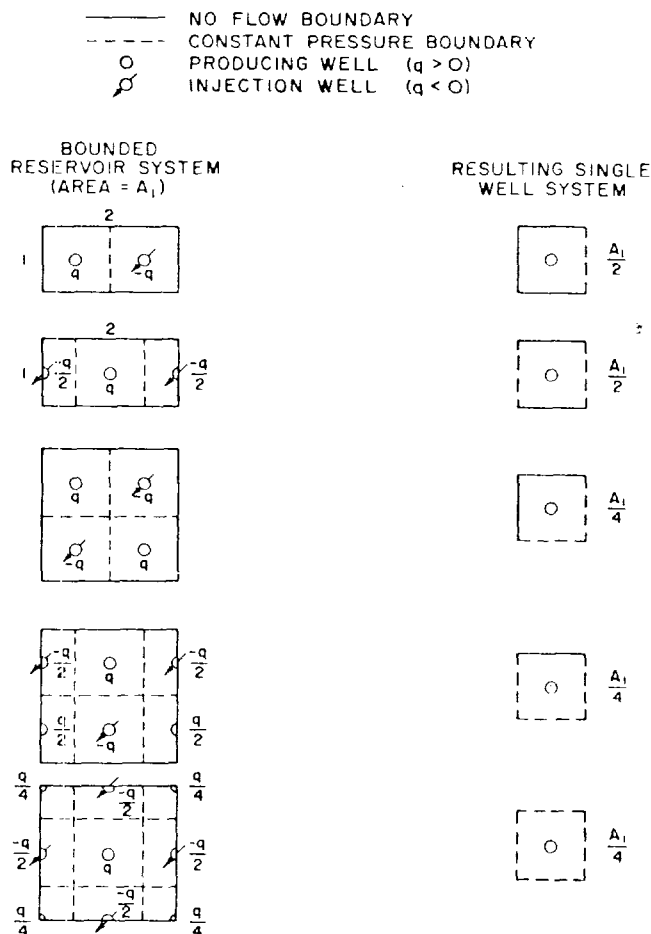


Fig. 8—Generation of drainage areas with constant pressure boundaries

Conclusions

In principle, the unsteady solution for a cylindrical, constant rate source (or sink) in an infinite medium can be used to generate, by superposition, solutions for almost any type of geometrical reservoir shape. However, these solutions may be obtained more easily by using the solution for a square with a single well in the center as a building block for superposition.

The unsteady pressure behavior has been computed at the well and at various other points for a square, bounded drainage region with the well at the center. Results of this computation provide the basis for the superposition mentioned above.

Of a large variety of potential applications, only a few have been shown. These include generation of the Matthews-Brons-Hazebroek pressure buildup corrections for various geometrical shapes (thus, pseudo-steady-state shape factors) and generation of dimensionless pressure distributions for production at constant rate, both for closed and for constant-pressure outer boundary conditions. The extension of this to a variety of geometrical shapes has been outlined.

Other potential applications include generation of the behavior of multiwell geometric reservoir shapes for wells producing at variable rates, and water influx reservoir behavior calculations for aquifer geometries other than circular and linear.

One of the significant realizations of this study was the usefulness of knowledge of the behavior of the square drainage region.

Nomenclature

a_i = distance from point x_m, y_m to the i th image well (Eq. 7)

$a_{im} = a_i/\sqrt{A}$

A = area of drainage region

c = compressibility

C_A = shape factor (Eq. 15)

h = formation thickness

k = permeability

L = half length of the side of the square = $\sqrt{A}/2$

p = pressure

p_D = dimensionless pressure as defined by Eq. 2

$p_{D\text{MATH}}$ = dimensionless pressure as defined by Matthews, Brons and Hazebroek (Eq. 10)

$p_{D\text{MILL}}$ = dimensionless pressure as defined by Miller, Dyes and Hutchinson

p_i = initial ($t = 0$) pressure

p_{ws} = bottom-hole pressure at any time after shut-in

\bar{p} = average pressure of drainage region

p^* = pressure at infinite shut-in time, extrapolated from buildup plot

q = volumetric production rate at reservoir conditions; positive: production, negative: injection

r = radial distance from a well

r_D = dimensionless radial distance = r/r_w

r_w = wellbore radius

t = time

t_D = dimensionless time based on wellbore radius (Eq. 4)

t_{DA} = dimensionless time based on drainage area (Eq. 8)

x_D = dimensionless x coordinate (Eq. 13)

y_D = dimensionless y coordinate (Eq. 14)

ϕ = porosity

μ = viscosity

Acknowledgments

The computing time needed for this study was made available by both Stanford U. and Marathon Oil Co. The authors gratefully acknowledge this assistance.

References

1. van Everdingen, A. F. and Hurst, W.: "The Application of the Laplace Transformation to Flow Problems in Reservoirs", *Trans., AIME* (1949) Vol. 186, 305-324.
2. Chatas, A. T.: "A Practical Treatment of Nonsteady-State Flow Problems in Reservoir Systems", *Pet. Eng.* (1953) Vol. 25, No. 5, B42; Vol. 25, No. 6, B38; Vol. 25, No. 9, B44.
3. Mortada, M.: "A Practical Method for Treating Oilfield Interference in Water-Drive Reservoirs", *Trans., AIME* (1955) Vol. 204, 217-226.
4. Katz, D. L., Tek, M. R., Coats, K. H., Katz, M. L., Jones, S. C. and Miller, M. C.: *Movement of Underground Water in Contact with Natural Gas*, AGA, New York (Feb., 1963) 251-271.
5. Mueller, T. D. and Witherspoon, P. A.: "Pressure Interference Effects Within Reservoirs and Aquifers", *J. Pet. Tech.* (April, 1965) 471-474.
6. Matthews, C. S., Brons, F. and Hazebroek, P.: "A Method for Determination of Average Pressure in a Bounded Reservoir", *Trans., AIME* (1954) Vol. 201, 182-191.
7. Theis, C. V.: "The Relationship Between the Lowering of the Piezometric Surface and the Rate and Duration of Discharge Using Ground Water Storage", *Trans., AGU* (1935) 519.
8. Brons, F. and Miller, W. C.: "A Simple Method for Correcting Spot Pressure Readings", *J. Pet. Tech.* (Aug., 1961) 803-805.
9. Dietz, D. N.: "Determination of Average Reservoir Pressure from Build-Up Surveys", *J. Pet. Tech.* (Aug., 1965) 955-959.
10. Muskat, M.: *The Flow of Homogeneous Fluids Through Porous Media*, J. W. Edwards, Inc., Ann Arbor, Mich. (1946) 587.
11. Ramey, H. J., Jr.: "Application of the Line Source Solution to Flow in Porous Media — A Review", *Prod. Monthly* (May, 1967) 4.
12. Miller, C. C., Dyes, A. B. and Hutchinson, C. A.: "Estimation of Permeability and Reservoir Pressure from Bottom-hole Pressure Build-up Characteristics", *Trans., AIME* (1950) Vol. 189, 91-104. ★★★

CALCULATION OF MAXIMUM
ALLOWABLE PRESSURE INCREASE
AT CARTER NO. 1

Equivalent depth of top Freeman ACF No. 1 disposal zone in the
Carter No. 1 = 10,000 feet

Naturally occurring pressure in disposal zone = 3,410 psi
From DST 10,160-10,198 feet in Magnolia Pet. Co.
Shipp No. 1 located 1980 feet FS&WL Sec.22,T.16S.,
R.37E.

Water Specific Gravity = 1.08 => 9 lb./gal.

Depths of potential fresh water zones in Carter No. 1:

Ogollala at 275 feet

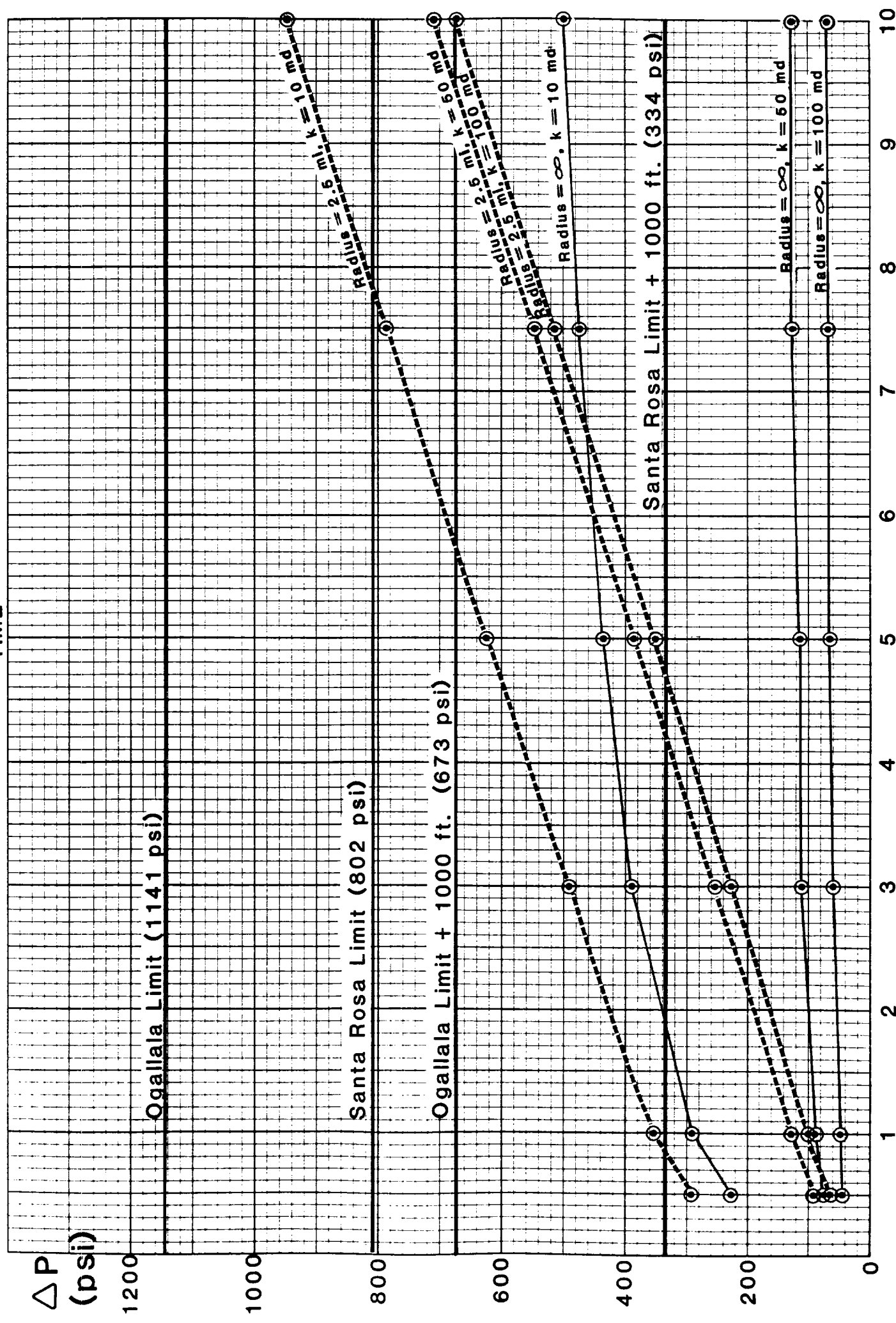
Santa Rosa at 1000 feet

NOTE: This is a low probability water zone and is based
solely on brackish water encountered while drilling the
Phillips YX State No. 1 in Sec.36,T.15S.,R.36E. This
well is located approximately five miles North of the
Carter No. 1.

VARIOUS POSSIBLE FLUID LEVEL LIMITS

- (1). Ogollala at 275 feet
Fluid Column = 10,000 - 275 = 9,725 feet
Pressure To Lift Column = 9,725 x 9 x .052 = 4,551 psi
Allowable Pressure Increase = 4,551 - 3,410 = 1,141 psi
- (2). Ogollala plus 1,000 at 1,275 feet
Fluid Column = 10,000 - 1,275 = 8,725 feet
Pressure To Lift Column = 8,725 x 9 x .052 = 4,083 psi
Allowable Pressure Increase = 4,083 - 3,410 = 673 psi
- (3). Santa Rosa at 1,000 feet
Fluid Column = 10,000 - 1,000 = 9,000 feet
Pressure To Lift Column = 9,000 x 9 x .052 = 4,212 psi
Allowable Pressure Increase = 4,212 - 3,410 = 802 psi
- (4). Santa Rosa plus 1,000 at 2,000 feet
Fluid Column = 10,000 - 2,000 = 8,000 feet
Pressure To Lift Column = 8,000 x 9 x .052 = 3,744 psi
Allowable Pressure Increase = 3,744 - 3,410 = 334 psi

VS
TIME



Attachment 8

Amerind Oil

Carter #1

Sec. 28-T16S-R37E

810' FNL & 660' FEL

Permo Penn

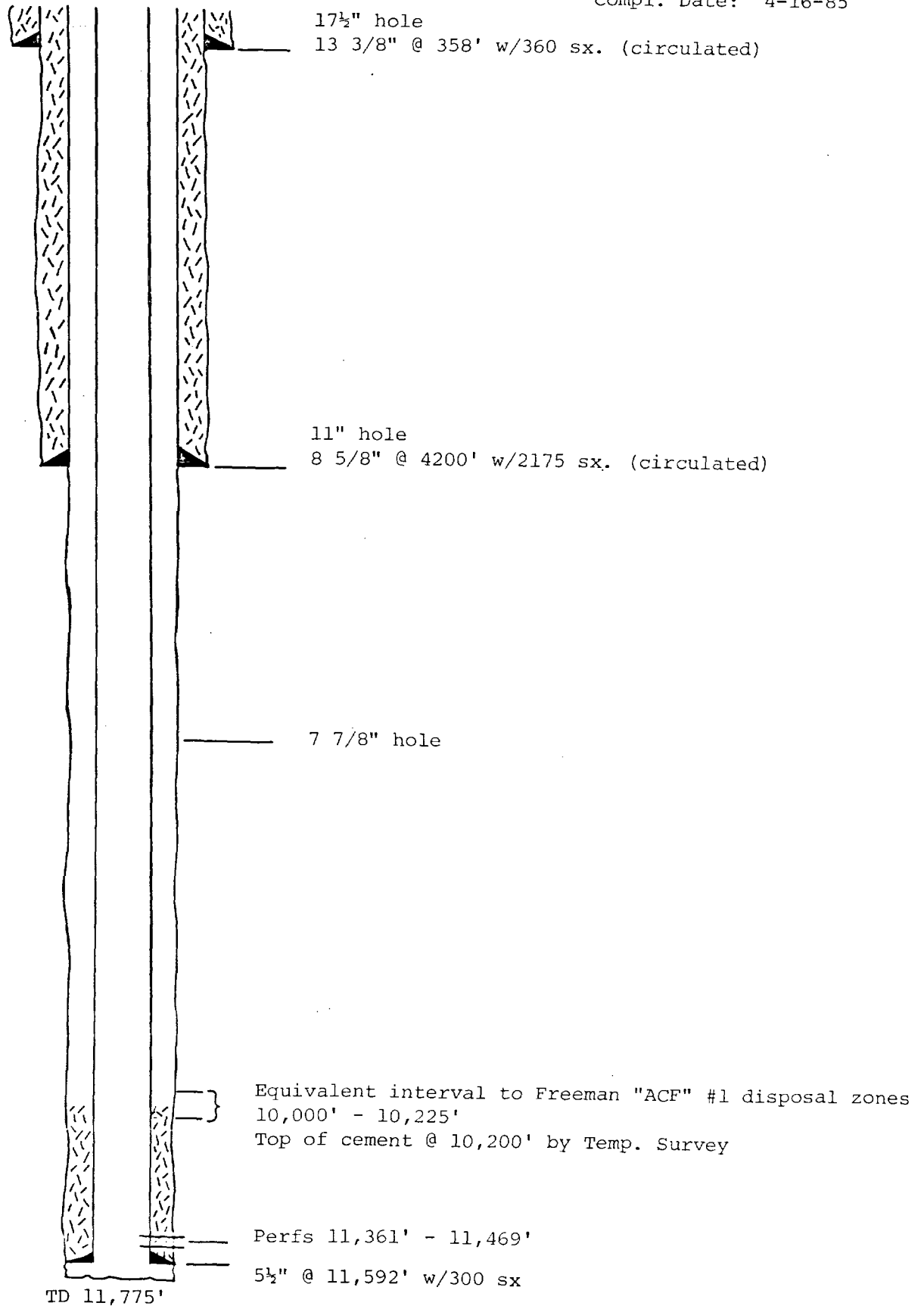
Lea County, New Mexico

Spud Date: 2-28-85

Compl. Date: 4-16-85

Elev. 3802' KB

3788' GL





105 SOUTH FOURTH STREET
ARTESIA, NEW MEXICO 88210
TELEPHONE (505) 748-1471

S. P. YATES
PRESIDENT
JOHN A. YATES
VICE PRESIDENT
B. W. HARPER
SEC. - TREAS.

December 11, 1986

TO: Offset Mineral Interest Owners

RE: Freeman ACF No. 1
660' FSL & 660' FWL
Sec.22,T.16S.,R.37E.
Lea County, New Mexico

Gentlemen:

On August 28, 1986, the New Mexico Oil Conservation Division approved the referenced well for salt water disposal by Order No. R-8290. The Order limits surface injection pressure to 500 psi, but contains a provision for the Director of the Division to administratively approve raising the pressure limit.

Yates Petroleum Corporation is now seeking the Director's approval of a higher pressure limit. A step rate test has been conducted to determine formation fracture pressure. The new pressure limit requested will be less than the fracture pressure.

If you have any comments or questions, please feel free to contact me at (505)748-1471.

If you have any objection to these plans, please notify the New Mexico Oil Conservation Division, P.O. Box 2088, Santa Fe, New Mexico 87504-2088.

Thank you for your continued cooperation.

Sincerely,

Albert R. Stall
Engineer

cc: N.M.O.C.D., Santa Fe
N.M.O.C.D., Hobbs

OFFSET OPERATORS

Township 16 South, Range 37 East, NMPM
Lea County, New Mexico

Pennzoil Exp. and Prod. Co.
P.O. Box 1828
Midland, TX 79701
ATTN: Land Dept.

Moncor Trust Co., Trustee
for W.T. Reed
P.O. Box 70
Hobbs, NM 88240
ATTN: Ms. Terry Howard

Jeanne Van Zant Sanders
Sinclair Bldg., Suite 508
106 W. Fifth Street
Fort Worth, TX 76102

Harry J. Schafer, Jr., Trustee
P.O. Box 14667
Oklahoma City, OK 73113

Sun Exploration and Prod. Co.
P.O. Box 1861
Midland, TX 79702

Bill Seltzer
507 Petroleum Bldg.
Midland, TX 79701

Texaco, U.S.A.
P.O. Box 3109
Midland, TX 79701
ATTN: Land Dept.

Mr. James R. McCrory
P.O. Box 25764
Albuquerque, NM 87125

Petco Limited
P.O. Box 911
Breckenridge, TX 76024

Coates Energy Trust and
Elizabeth H. Maddux
P.O. Box 171717
San Antonio, TX 78217

J.H. Van Zant, II
1722 Commerce Bldg.
307 W. 7th
Fort Worth, TX 76102

Amerind Oil Co.
500 Wilco Bldg.
Midland, TX 79701

Ensearch Exploration, Inc.
P.O. Box 4815
Midland, TX 79704
ATTN: Land Dept.

Mr. James R. Woods
P.O. Box 1417
Socorro, NM 87801

Mrs. Mary K. Grisso
2328 N.W. 47th
Oklahoma City, OK 73112

Felmont Oil Corporation
P.O. Box 2266
Midland, TX 79702

Heritage Resources
Paragon Tower, Suite 1000
600 N. Marienfield St.
Midland, TX 79701

American Quasar Pet. Co.
One First City Center
Suite 1000
Midland, TX 79701